Paleoceanography and Paleoclimatology

RESEARCH ARTICLE
10.1029/2024PA004843

Western Pacific Warm Pool Warming and Salinity Front Expansion Since 1821 Reconstructed From Paired Coral $\delta^{18}O$, Sr/Ca, and Reconstructed $\delta^{18}O_{sw}$

Sara Todorović[1,2], Henry C. Wu[1], Braddock K. Linsley[3], Henning Kuhnert[4], Christophe Menkes[5], Albina Isbjakowa[1], and Delphine Dissard[6]

[1]Leibniz Centre for Tropical Marine Research (ZMT), Bremen, Germany, [2]Faculty of Geosciences, University of Bremen, Bremen, Germany, [3]Lamont-Doherty Earth Observatory of Columbia University, Palisades, NY, USA, [4]MARUM – Center for Marine Environmental Sciences, University of Bremen, Bremen, Germany, [5]ENTROPIE (IRD, University of New Caledonia, University of La Réunion, CNRS, Ifremer), Nouméa, New Caledonia, [6]LOCEAN (IRD-CNRS-MNHN-Sorbonne Universités), Nouméa/Paris, France

Abstract The Southwest Pacific region is of great importance to global climate variability, but instrumental climate observations before the 1980s lack in numbers and quality. Despite efforts in complementing instrumental records with proxy sea surface temperature (SST) and sea surface salinity (SSS) reconstructions based on coral Sr/Ca and $\delta^{18}O_{sw}$ records, few of them are longer than a century. This study introduces a northwestern extension to the existing records of South Pacific coral study sites with monthly-resolved Sr/Ca, $\delta^{18}O$, and $\delta^{18}O_{sw}$ reconstructions from Rotuma dating back to 1821. Additionally, we present new monthly-resolved Sr/Ca and reconstructed $\delta^{18}O_{sw}$ from a coral from Tonga dating back to 1848. Results reveal 1.5°C warming in the Western Pacific Warm Pool, while the adjacent coral from Tonga shows 1°C warming over the twentieth century. The Rotuma Sr/Ca record reveals thermal stress events impacting the Sr/Ca-SST relationship in the following months. Coral $\delta^{18}O_{sw}$ results reveal significant freshening of 0.45 S_p (practical salinity unit) in Tonga since the early twentieth century, suggesting the southeastward expansion of the South Pacific Convergence Zone salinity front. The $\delta^{18}O_{sw}$ inferred SSS provides a valuable extension into the past considering the short and inconsistent instrumental records available. This study demonstrates the utility of coral-based reconstructions in capturing long-term and regional climate variations in the Southwest Pacific and the necessity of expanding replicated studies to other underrepresented areas to enhance our understanding of regional climate dynamics.

Plain Language Summary The Southwest Pacific has limited historical climate data. This makes studying anthropogenic climate change, and how it is changing our oceans, very challenging. This study addresses this gap by using massive tropical corals from Rotuma and Tonga to reconstruct climatic key parameters back to the mid-1800s. Our findings show that the Western Pacific Warm Pool (WPWP) has warmed by 1.2°C, much more than the adjacent subtropical waters around Tonga (0.5°C) between 1850 and 1998. The Rotuma coral record is one of the rare long records from the WPWP area where the average annual temperatures are very high (29°C). It reveals the coral was repeatedly affected by temperature stress, and probably unreported bleaching episodes throughout history. We also observe a significant freshening of 0.45 S_p in Tonga, indicating that fresher waters from the South Pacific Convergence Zone are spreading southeastward. Our coral-derived records provide valuable historical perspectives in the absence of consistent instrumental records. Our study emphasizes the reliability of coral-based reconstructions as indicators of local to regional conditions in the Southwest Pacific and the need for more research to better understand and address climate variability of this key area for Pacific-wide climate.

Key Points:

- Rotuma coral Sr/Ca and $\delta^{18}O_{sw}$ records provide the first reconstructions of surface seawater temperature and salinity from this location
- Coral Sr/Ca-SST shows long-term warming in the Southwest Pacific, with higher rates in the Western Pacific Warm Pool, compared to subtropics
- $\delta^{18}O_{sw}$-SSS reconstruction from Tonga shows significant long-term freshening

Supporting Information:

Supporting Information may be found in the online version of this article.

Correspondence to:

S. Todorović and H. C. Wu,
sara.todorovic@leibniz-zmt.de;
henry.wu@leibniz-zmt.de

Citation:

Todorović, S., Wu, H. C., Linsley, B. K., Kuhnert, H., Menkes, C., Isbjakowa, A., & Dissard, D. (2024). Western Pacific warm pool warming and salinity front expansion since 1821 reconstructed from paired coral $\delta^{18}O$, Sr/Ca, and reconstructed $\delta^{18}O_{sw}$. *Paleoceanography and Paleoclimatology*, *39*, e2024PA004843. https://doi.org/10.1029/2024PA004843

Received 9 JAN 2024
Accepted 1 OCT 2024

Author Contributions:

Conceptualization: Sara Todorović, Henry C. Wu
Data curation: Henning Kuhnert, Albina Isbjakowa
Formal analysis: Sara Todorović
Funding acquisition: Henry C. Wu
Methodology: Sara Todorović, Henning Kuhnert
Project administration: Henry C. Wu
Resources: Braddock K. Linsley, Christophe Menkes, Delphine Dissard
Supervision: Henry C. Wu
Visualization: Sara Todorović, Christophe Menkes
Writing – original draft: Sara Todorović

1. Introduction

The Southwest Pacific (SW Pacific) plays a crucial role in global and Pacific-wide climate patterns. However, the region still has consequential deficiencies in climate observations dating back more than a few decades (Brown et al., 2020; Dutheil et al., 2022). One of the key features of the region is the South Pacific Convergence Zone (SPCZ), which is a permanent spur of the Intertropical Convergence Zone spanning from the Western Pacific Warm Pool (WPWP) southeastwards to the subtropics (Brown et al., 2020; Trenberth, 1976) (Figure 1a). The SPCZ is a key driver of precipitation variability in the Southern Hemisphere (Folland et al., 2002; Salinger

Writing – review & editing:
Sara Todorović, Henry C. Wu, Braddock K. Linsley, Henning Kuhnert, Christophe Menkes, Albina Isbjakowa, Delphine Dissard

et al., 1995). Characterized by intense rainfall and permanent cloudiness, the SPCZ is a major contributor to the regional cyclogenesis (Vincent et al., 2011). Changes in sea surface temperature (SST) and rainfall in the SW Pacific may lead to regional flooding, drought, and extreme weather affecting island communities (Kuleshov et al., 2014; McGree et al., 2016). The seasonal pattern and intensity of precipitation affect regional sea surface salinity (SSS) variability, while the annual to interannual processes of climate variability affect the position of the SPCZ salinity front (Singh et al., 2011). The salinity front separates the low-salinity waters of the warm and fresh pool from the saltier and cooler subtropical waters. The WPWP also plays an important role in climate dynamics of the region as it generates a considerable amount of heat energy (D'Arrigo et al., 2006). Variability of the WPWP extent and intensity also influences the Walker Circulation (Liu & Huang, 1997), East Asian monsoon (Chongyin et al., 1999) and is tightly linked to the CO_2 radiative forcing (Peter et al., 2023; Tachikawa et al., 2014). Currently, the available SST and SSS data sets and gridded products struggle to capture local coastal processes for many small islands of the SW Pacific due to the products' coarse resolution, which could misrepresent trends in such variable environments. Highly resolved coral-based reconstructions of SST and SSS provide the necessary longer-term perspective for describing past local and regional oceanographic variability of regions with sparse observational data coverage.

1.1. Scleractinian Corals as Climate Recorders

Coral-based reconstructions of SST and SSS from massive tropical corals such as *Porites* sp. have been extensively used to complement and extend the available observational data and describe the natural conditions of the South Pacific (Bagnato et al., 2005; Corrège, 2006; Dassié et al., 2014, 2018; Juillet-Leclerc et al., 2006; Le Bec et al., 2000; Linsley et al., 2004, 2006, 2008, 2015; Quinn et al., 2006; Tangri et al., 2018; Wu et al., 2013). Most available coral-based reconstructions of climate parameters are based on skeletal $\delta^{18}O$, which is influenced by both SST and $\delta^{18}O$ of seawater ($\delta^{18}O_{sw}$). Both parameters are influenced by fresh water admixture and evaporation processes (Fairbanks et al., 1997; LeGrande & Schmidt, 2006). In the Pacific, the corals are especially hydrosensitive due to intense convection and high rates of precipitation leading to a bigger portion of $\delta^{18}O$ variance being driven by $\delta^{18}O_{sw}$, thus making for a stronger case for Sr/Ca-based SST reconstructions from massive corals (Fairbanks et al., 1997; Thompson et al., 2022). Due to its long residence time of 4 My and minor depth gradients, the variability of the Sr to Ca ratio is low in oligotrophic surface waters, and relatively stable on timescales of a few centuries used in coral-based reconstructions (Lebrato et al., 2020; de Villiers et al., 1994). While in abiogenic precipitation experiments, there is a clear dependence of Sr/Ca to temperature (DeCarlo et al., 2015), seasonal fluctuations in aragonite precipitation efficiency or Rayleigh fractionation can affect Sr/Ca ratios in corals in addition to temperature (Gaetani & Cohen, 2006). However, there is no dependence between a range of growth rates and Sr/Ca (Alibert & McCulloch, 1997; Mitsuguchi et al., 2003), and the Rayleigh model doesn't explain Sr/Ca variability when precipitating from a seawater-like fluid (Inoue et al., 2015). The Sr/Ca-SST relationship varies between coral colonies (Alpert et al., 2016; Cahyarini et al., 2009; Linsley et al., 2006; Pfeiffer et al., 2009) and is highly dependent on the underlying SST data set and method used for establishing calibration (Corrège, 2006). While the generally accepted coral Sr/Ca-SST sensitivity converges around -0.06 mmol $mol^{-1}°C^{-1}$ (Corrège, 2006), there is some evidence that rescaling to steeper slopes is needed to increase the sensitivity and accuracy of SST reconstructions (e.g., Gagan et al., 2012, -0.084 mmol/mol $°C^{-1}$). Despite the generally established application of the Sr/Ca-SST proxy and its robustness, its fidelity can be affected by physiological processes associated with calcification or stressful events (Cheung et al., 2021; Clarke et al., 2019; DeCarlo & Cohen, 2017; D'Olivo et al., 2019; Marshall & McCulloch, 2002; Schoepf et al., 2021). Particularly in stressful environmental conditions, such as heat stress events and bleaching episodes, the disruption of metabolic and calcification processes can lead to the disruption of the Sr/Ca-SST relationship, sometimes lasting multiple years (Cheung et al., 2021; D'Olivo et al., 2019). One of the benefits of having paired coral $\delta^{18}O$ and Sr/Ca data is the possibility to reconstruct $\delta^{18}O_{sw}$ by removing the temperature contribution in coral $\delta^{18}O$ (e.g., Cahyarini et al., 2008; Ren et al., 2002). In the tropics, $\delta^{18}O_{sw}$ has been shown to be well correlated to SSS (Fairbanks et al., 1997; Schmidt, 1999), which may provide a more accurate SSS reconstruction compared to $\delta^{18}O$-SSS based on a single proxy.

Sr/Ca-based SST reconstructions of the SW Pacific show secular, nonlinear warming trends since the 1900s and indicate the WPWP expansion and southward shift of the South Pacific gyre (e.g., Wu et al., 2013). Reconstructed $\delta^{18}O_{sw}$ from Tonga, Fiji, and Rarotonga corals support the long-term freshening trend and southward displacement of the SPCZ (Linsley et al., 2006; Wu et al., 2013). Moreover, SSS reconstructions based on coral

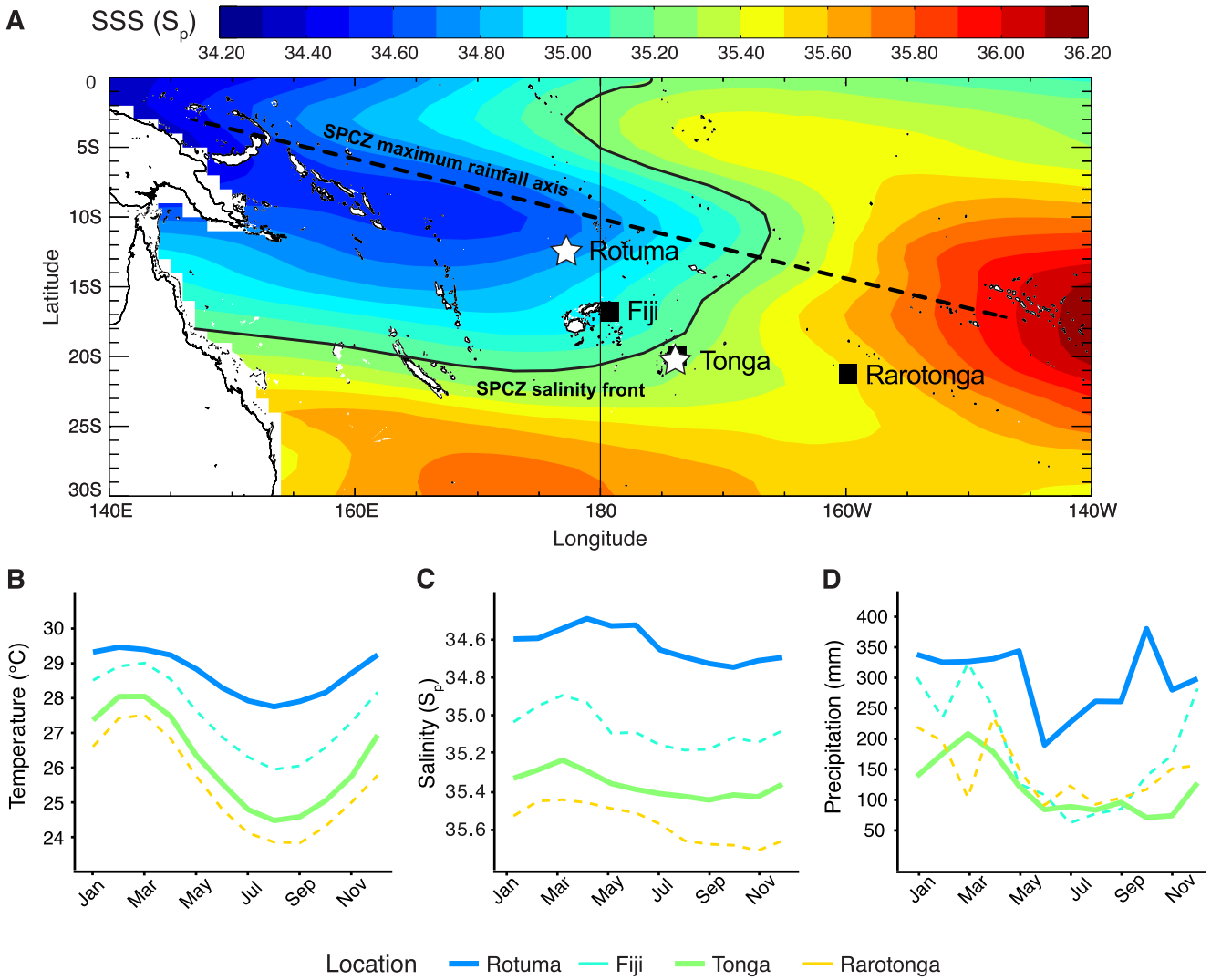

Figure 1. (a) Map of the SW Pacific shaded with Delcroix 1° × 1° sea surface salinity (SSS) data set means for the climatology period, mean maximum precipitation axis of the South Pacific Convergence Zone (SPCZ) (Brown et al., 2020) is shown with the dashed black line, and the 35.2 S_p isohaline delineates the mean extent of the SPCZ and the salinity front with a solid black contour. Corals presented in this study are marked with stars, with locations of other regional coral reconstructions marked with squares; (b) Average SSTs are calculated from OISST 1° × 1° (Reynolds et al., 2002); (c) Average SSS are calculated from Delcroix et al. (2011), grid cells for centering are available in Table S1 in Supporting Information S1; (d) Average precipitation are calculated from the PACRAIN database (Greene et al., 2008), grid cells for centering are available in Table S1 in Supporting Information S1. Locations of corals presented in this study are presented with bold lines. All climatology is based on the period from 1981 to 1995.

$\delta^{18}O$ show gradual eastward displacement of the SPCZ salinity front in the last 200 years suggesting expansion of the SPCZ fresh pool (Dassié et al., 2018; Wu et al., 2013). The lack of significant total precipitation trends in the SPCZ since the mid-twentieth century (Griffiths et al., 2003) and concurrent expansion of the WPWP area (Roxy et al., 2019) point to ocean dynamics having the dominant role in the freshening trend in the region. However, studies also show ocean dynamics and atmospheric feedbacks in the region are complex and especially in response to increasing temperatures from rising CO_2 emissions (Heede et al., 2021; Seager et al., 2019; Seager & Murtugudde, 1997). This emphasizes the need for replicated proxy records to further our understanding of paleoclimatic variations and their nonhomogeneous pattern across the SPCZ.

1.2. Study Area

Rotuma, a Fijian dependency, is a small volcanic island located ~500 km northwest of the main Fijian islands of Viti Levu and Vanua Levu (Figure 1a). Rotuma exhibits an average annual SST of 28.7°C that places it within the

WPWP with a small seasonal SST amplitude of only 1.7°C based on the 1° by 1° gridded Optimum-Interpolated SST (OISST) centered on the grid 12.5° S and 176.5° E between 1981 and 1995 (Reynolds et al., 2002) (Figure 1b). The average annual SSS of 34.7 Practical Salinity (S_p) for the same period places Rotuma within the SPCZ salinity front isohaline of 35.2 S_p, with seasonal cycles of 0.3 S_p, which on interannual timescale shows much higher variability of up to 2.0 S_p (Figure 1c). On average, the island receives around 3,500 mm of annual precipitation, mostly during austral winter (August-October) and around March/April (Greene et al., 2008). The wet season leads to secondary cooling within the annual cycle during austral summer with an appearance of multiple SST increases and decreases within a single year (see Figure S2 in Supporting Information S1).

Tonga islands are located around 1,200 km southeast of Rotuma (Figure 1a). They spread in an arc following the volcanically active convergent margins of the Indo-Australian and Pacific tectonic plates. Nomuka Iki is a limestone island of reef origin, located on the eastern part of the arc characterized by abundant and well-developed coral reefs. Compared to Rotuma, the annual average SST is lower (26.2°C), and the average seasonal amplitude increases to 3.6°C based on the 1° by 1° gridded OISST centered on the grid 19.5° S and 174.5° W (Reynolds et al., 2002) (Figure 1b). Compared to Rotuma, the annual SSS of Tonga is higher at 35.4 S_p with a smaller seasonal cycle of 0.2 S_p, and the interannual variability decreases to 1.5 S_p. The precipitation pattern of Tonga has a distinct rainy season from June to October and receives less than half the annual precipitation of Rotuma at 1,500 mm overall.

The geographical locations of the two islands exhibit large gradients of SST and SSS along the diagonal extension of the SPCZ (Figures 1b–1d), thus providing unique climatological insights into the region.

1.3. Aims of the Study

To address the gap in climate reconstruction in the WPWP and along the SPCZ axis, and to better describe the oceanographic variability of the SPCZ, we introduce new monthly resolved coral-based reconstructions from Rotuma, a Fijian dependency, and Nomuka Iki, Kingdom of Tonga. Covering the period from 1821 to 2004, these coral records describe the coral responses to oceanographic variability in the WPWP and along the SPCZ axis, contributing new insights to these under-sampled regions. We use monthly-resolved paired $\delta^{18}O$ and Sr/Ca from the two corals to infer SSS variability at the two locations based on the reconstruction of $\delta^{18}O_{sw}$.

2. Methods

2.1. Coral Collection and Micro-Sampling

The coral core from the island of Rotuma (RO2) (12° 29′ S; 177° 06′ E) was retrieved from a living *Porites* sp. colony at 11 m water depth in October 1998 during the PALEOTUVALU cruise. The total core length retrieved is 2.35 m. The RO2 coral core was cut into 7 mm thick slabs and cleaned with 18.2 MΩ milli-Q water in an ultrasonic bath for 5 minutes on each side, repeating until the water was clear, and then air dried. X-radiographs of the slabs were used to identify the maximum growth axis based on density banding for millimeter (mm) sampling (Figure S1 in Supporting Information S1). Preliminary analyses of the slabs exhibit no external intrusions, borings, or unusual skeletal patches. Petrographic thin sections show no diagenesis including secondary aragonite development. The slabs were sampled with a 0.5 mm drill bit, using a handheld Proxxon drill, in continuous 1-mm increments along the maximum growth axis to obtain close to monthly resolution based on the average rate of vertical linear extension of 10 ± 2.5 mm per year. The powder coral skeletal material was analyzed for $\delta^{18}O$ and Sr/Ca.

Coral TNI2 from Tonga was collected in November 2004, from a living *Porites lutea* colony at Nomuka Iki (20° 16′ S, 174° 49′ W) at 3.5 m water depth. Details of the micro-sampling, chronology determination, and the skeletal $\delta^{18}O$ record were previously discussed (Linsley et al., 2008). For Sr/Ca analyses, we have re-sampled the coral slab parallel and adjacent to the original sampling track using the same continuous mm increment micro-sampling method. Trace elements analysis of TNI2 was completed in every other mm resolution to match the previously published analytical resolution (Linsley et al., 2008). In addition to the time series of skeletal Sr/C, reconstructed $\delta^{18}O_{sw}$ from the core TNI2 from Tonga are presented for the first time, based on the previously published $\delta^{18}O$ time series (Linsley et al., 2008).

2.2. Geochemical Analysis

Coral skeletal $\delta^{18}O$ signature was measured from individual powders at the MARUM, University of Bremen, Germany, using a Thermo-Finnigan MAT 251 and MAT 253 gas isotope ratio mass spectrometer with Kiel I and Kiel IV automated carbonate preparation devices. All coral $\delta^{18}O$ results are reported as permil deviations relative to Vienna Peedee belemnite (‰ VPDB). Long-term internal reproducibility of the $\delta^{18}O$ signature was better than ±0.06‰ (1σ, $n = 623$) based on repeat measurements of an internal standard.

Trace elements were measured at the Leibniz Centre for Tropical Marine Research (ZMT), ICP-MS Lab, Bremen, Germany on the Analytik Jena PlasmaQuant MS Elite Inductively Coupled Plasma Mass Spectrometer following the method modified from (Schrag, 1999) adapted for our instrument. Briefly, each homogenized powder sample was weighed into 500 µg subsamples and dissolved in 2 ml supra pure Optima grade 2% HNO_3 in acid-cleaned 2 ml micro-centrifuge tubes. The samples were further diluted for analysis to achieve approximately 50 ppm Ca concentration. The analytical procedure had the coral samples bracketed by (a) a stock solution standard mixed with single elemental standards replicating the trace element concentrations of the JCp-1 coral standard (Okai et al., 2002) after each sequence of five samples. Additionally, (b) the JCp-1 coral standard and (c) an internal coral standard were measured after each sequence of 10 coral samples. Acid blanks were routinely measured to check for contamination. Counts per second (cps) data were converted to concentrations and drift corrected using a calibration based on five standards and one blank. Calibration standards were diluted from the stock solution standard. To account for potential laboratory-specific offsets and inter-daily variability, the data were further corrected for the difference between measured and published values for JCp-1 (Hathorne et al., 2013). Long-term internal reproducibility of Sr/Ca was better than ±0.03‰ (1σ, $n = 503$) for RO2 and ±0.02‰ (1σ, $n = 305$) for TNI2 based on repeated measurements of JCp-1. For the coral RO2, a total of 1776 samples (1924 including sampling track change overlaps) were analyzed for $\delta^{18}O$ and Sr/Ca, and a total of 1154 TNI2 samples were analyzed for Sr/Ca.

2.3. Coral Chronology Development

The RO2 chronology was established based on annual density banding when it was clearly visible (Figure S1 in Supporting Information S1) and aided by the observed $\delta^{18}O$ seasonality in less distinct sections. We chose $\delta^{18}O$ for chronology development as it showed clear seasonal cycles compared to Sr/Ca with irregular seasonality observed in some years, possibly influenced by the small and irregular seasonal cycle observable in the SST (Figure S3a in Supporting Information S1). The RO2 Sr/Ca and $\delta^{18}O$ were both measured on the same mm samples and therefore share the same chronology. Due to multiple changes in natural polyp growth direction, the sampling tracks were occasionally changed. Old and new tracks ran parallel over a length of about 1 cm. The overlap allowed for the splicing of the $\delta^{18}O$ and Sr/Ca values from both paths into single continuous records. The slab breaks of this core were clean and without considerable material loss, and the final record is deduced to be free of hiatuses.

Months with the highest (most commonly February/March) and lowest SST (August) were tied to coral $\delta^{18}O$ minimum and maximum values within each annual density band, respectively. OISST 1° × 1° was used (Reynolds et al., 2002) to set the seasonal cycle tie-points. Both instrumental data and coral $\delta^{18}O$ exhibit noisy time series due to the seasonal SST cycle being influenced by the dry and wet seasons. This resulted in anomalously warm months in austral winter, and cool months in austral summer which create double highs and lows being ubiquitous in this SST time series. These double decreases in SST (September/October) and peaks (January through April) (see Figure S3 in Supporting Information S1) were assigned to coinciding additional $\delta^{18}O$ maxima and minima respectively, wherever the temporal resolution was approximately monthly. In years of slower growth and with fewer data points (<6 $years^{-1}$), tie points were assigned to annual minima and maxima only. For the remainder of the record the values of minimum $\delta^{18}O$ were tied to the hottest month on average (February), and maximum $\delta^{18}O$ to the coolest (August). Additional tie points for double low and high $\delta^{18}O$ values were assigned to the most common months of their occurrence only where the number of data points for a given year permitted. Monthly age estimates were then linearly interpolated based on these tie points using the ARAND software package programs Ager and Timer (Howell et al., 2006) and span from 1821 to 1998. Chronology for TNI2 based on the published $\delta^{18}O$ signature (Linsley et al., 2008) was used for the Sr/Ca time series.

Table 1
Parameters Used in $\delta^{18}O_{sw}$ Reconstruction Following the Method of Ren et al., 2002

	Rotuma (RO2)	Tonga (TNI2)
$\delta^{18}O$ to SST (‰°C^{-1})	−0.19	−0.15
Sr/Ca to SST (mmol mol^{-1}°C^{-1})	−0.090	−0.083
Average $\delta^{18}O_{sw}$ (‰, LeGrande et al., 2006)	0.349	0.498

Note. ERSST was used for obtaining the regression slopes of proxies with temperature. The calibration period of coral data to ERSST was 1950–1998 for RO2 and 2004 for TNI2. The calibration period for $\delta^{18}O_{sw}$ to D-SSS was 1960–1998 for RO2, and 2004 for TNI2. The regressions are described fully in Table 2.

2.4. SST and SSS Reconstructions

Coral Sr/Ca-SST, $\delta^{18}O$-SSS and $\delta^{18}O$-SST regressions for RO2 and TNI2 were calculated with monthly interpolated coral data against the OISST 1° × 1°, ERSST 2° × 2°, version 4 (Huang et al., 2015), monthly averaged Daily-OISST 0.25° × 0.25°, version 2.1 (Huang et al., 2021) and Ocean Reanalysis of the twentieth Century (ORA-20C) SST (de Boisséson et al., 2018) to test responses of corals to more regional and local conditions (Table S4 in Supporting Information S1). Each instrumental data set was centered on the grid closest to the coral locations (Table S1 in Supporting Information S1), with the calibration periods spanning the overlapping periods of coral and instrumental data. Coral proxy and instrumental data were also interpolated into seasonal (JFM, AMJ, JAS, OND) and austral winter/summer (JASO, JFMA) records to compare effects on regressions (Table S5 in Supporting Information S1). Seasons were determined based on the SST means, minima, and maxima identified in the climatology presented in Figure 1. The Ordinary Least Squares linear regression (OLS) and the Reduced Major Axis (RMA) OLS methods with bootstrapping at the 95% level with 1999 repetitions were applied to facilitate the comparison between these records and previously published Sr/Ca-SST sensitivity relationships (Bagnato et al., 2005; Corrège, 2006; Linsley et al., 2008; Wu et al., 2013). To inspect the strength of the Sr/Ca and SST relationship through time, a rolling 24-month correlation was calculated between coral Sr/Ca and ERSST.

The $\delta^{18}O_{sw}$ reconstruction technique of Ren et al. (2002) based on the monthly interpolated coral $\delta^{18}O$ and Sr/Ca records was employed. This method, similar to the centering method (Cahyarini et al., 2008), is preferable for $\delta^{18}O_{sw}$ reconstructions in the South Pacific because SST and SSS ($\delta^{18}O_{sw}$) co-vary and introduce a bias with traditional linear regression reconstructions (Cahyarini et al., 2008; Gouriou & Delcroix, 2002).

For coral-based reconstruction of $\delta^{18}O_{sw}$ values, the most recent gridded values of $\delta^{18}O_{sw}$ for each location were used (LeGrande & Schmidt, 2006). We used the $\delta^{18}O$ to SST (‰°C^{-1}) slope obtained from OLS regression, and Sr/Ca to SST (mmol mol^{-1}°C^{-1}) obtained from RMA regression, as discussed later in the text (regressions are presented in Table 2). The parameters used are listed in Table 1.

The $\delta^{18}O_{sw}$ reconstructions were then used as proxies of SSS for comparison to instrumental SSS data. We used monthly SSS products from the Simple Ocean Data Assimilation (SODA ver.2.2.4) (Carton & Giese, 2008), ORA-20C SSS (de Boisséson et al., 2018) and Delcroix et al. (2011) SSS, from here on abbreviated with D-SSS. All SSS data sets were centered on the grid cell closest to each coral core (see Table S1 in Supporting Information S1). The Delcroix data set was used as the SSS data set of choice in previous studies of the South Pacific region (Dassié et al., 2018; Tangri et al., 2018) because it offers a better spatial coverage of the region.

To determine the contributions of SST and SSS to the coral $\delta^{18}O$ values in Rotuma and Tonga, we produced a forward model of $\delta^{18}O_{coral\ (c)}$ for each location using the method of Thompson et al. (2011) and Equation 1:

Table 2
Calibration Relationships and Regression Equations for Sea Surface Temperature and Sea Surface Salinity Coral Proxies Against Instrumental Data

	$\delta^{18}O$ and ERSST (OLS)	r	Sr/Ca and ERSST (RMA)	r	$\delta^{18}O_{sw}$ and D-SSS (RMA)	r
RO2	−0.19 (±0.010) * SST − 0.46 (±0.292)	−0.61	−0.090 (±0.004) * SST + 11.42 (±0.105)	−0.21	0.60 (±0.025) * SSS − 20.16 (±0.868)	0.43
TNI2	−0.15 (±0.004) * SST − 0.79 (±0.098)	−0.84	−0.083 (±0.002) * SST + 11.14 (±0.045)	−0.84	0.47 (±0.020) * SSS − 16.06 (±0.688)	0.31

Note. Standard errors (±1σ) are shown in brackets. The calibration period of coral data to ERSST was 1950–1998 for RO2 and 2004 for TNI2. The calibration period for $\delta^{18}O_{sw}$ to D-SSS was 1960–1998 for RO2, and 2004 for TNI2. All results are significant at the $p < 0.0001$ level.

$$\delta^{18}O_{\text{pseudocoral}} = \alpha 1 \times \text{SST} + \alpha 2 \times \text{SSS} \quad (1)$$

ERSST and D-SSS for each location were used as SST and SSS sources. For the α1 and α2 constants of the pseudo-coral forward model, δ^{18}O-SST and $\delta^{18}O_{sw}$-SSS calibration slope values for each coral were used (Table 2).

To test for changes in mean and variance, change point analysis was performed on Sr/Ca and $\delta^{18}O_{sw}$ data with the seasonal component removed (and scaled for the changes in mean), using the changepoint package in R Statistical Software (Killick & Eckley, 2014; R Core Team, 2021). We used the At Most One Change method to identify changes in mean in secular trends, as well as the Pruned Exact Linear Time method to inspect the time series for multiple shifts corresponding to interdecadal forcings. Analyzing for significant shifts in mean is one of the more widely used change point methods for climate series (Beaulieu & Killick, 2018; Shi et al., 2022). The analysis identifies the maximum likelihood of a change point based on the data distribution and density and against a Bayesian information criterion penalty (Schwarz, 1978).

3. Results

3.1. Instrumental SST and SSS Comparison in the SPCZ

The comparison of four SST and three SSS reanalysis and model products for the two study locations revealed large incoherencies in variability between the data sets and locations. SST data over the 1981–1995 period show high r^2 values between each data set, or similarity, for the same location (Rotuma, r^2 = 0.79–0.91; Tonga, r^2 = 0.94–0.96). The SST data sets show strong agreement with each other, more so in Tonga compared to Rotuma where up to 20% of variability between different gridded SST products is sometimes not explained. The SSS data over the same period shows consistently low values (Rotuma, r^2 = 0.14–0.35; Tonga r^2 = 0.24–0.46) (Table S2 in Supporting Information S1), especially when the SODA data set is compared with other data sets. The variability explained between the SST data sets for the same location improves with a decrease of temporal resolution to seasonal or austral winter/summer which removes higher frequency noise. The variability explained between the SSS data sets, while showing improvement, remained consistently lower (Table S2 in Supporting Information S1).

3.2. Coral Proxy Calibrations

Since there are errors associated with both the coral proxy data and the instrumental data sets, RMA regression is favored over the commonly used OLS regression. Both regression styles were performed for our calibration to assist in comparison to previously published studies. We have chosen to take advantage of the RMA regression in the discussion of our Sr/Ca and $\delta^{18}O_{sw}$ results due to the lower spatial resolution of the ERSST data set used in the regressions, and because of the low coherence between the SSS data for each location (Table 2) (for OLS results, see Table S4 in Supporting Information S1).

Monthly coral δ^{18}O and Sr/Ca data are calibrated against ERSST for the benefit of extending further in time compared to the other data sets while maintaining a strong correlation (see Table S4 in Supporting Information S1). For $\delta^{18}O_{sw}$ to SSS calibration, we chose the D-SSS data set as it correlates better to both corals' data compared to the other SSS data available.

3.3. Coral Proxy Data

Monthly interpolated δ^{18}O and Sr/Ca data for both locations are shown in Figure 2. Secular trends in δ^{18}O reveal significant warming/freshening in both corals (Table 3).

3.3.1. δ^{18}O

Interannual variability is pronounced in the Rotuma coral δ^{18}O. The Tonga coral in comparison presents dominantly with a shift toward negative conditions around 1905–1915 (Linsley et al., 2008). Both corals exhibit well defined seasonal cycles in δ^{18}O, with Tonga having a higher seasonal amplitude (0.62‰) compared to Rotuma (0.34‰), which reflects the higher amplitude in local SST and SSS (Figures 1b and 1c, Table S3 in Supporting Information S1).

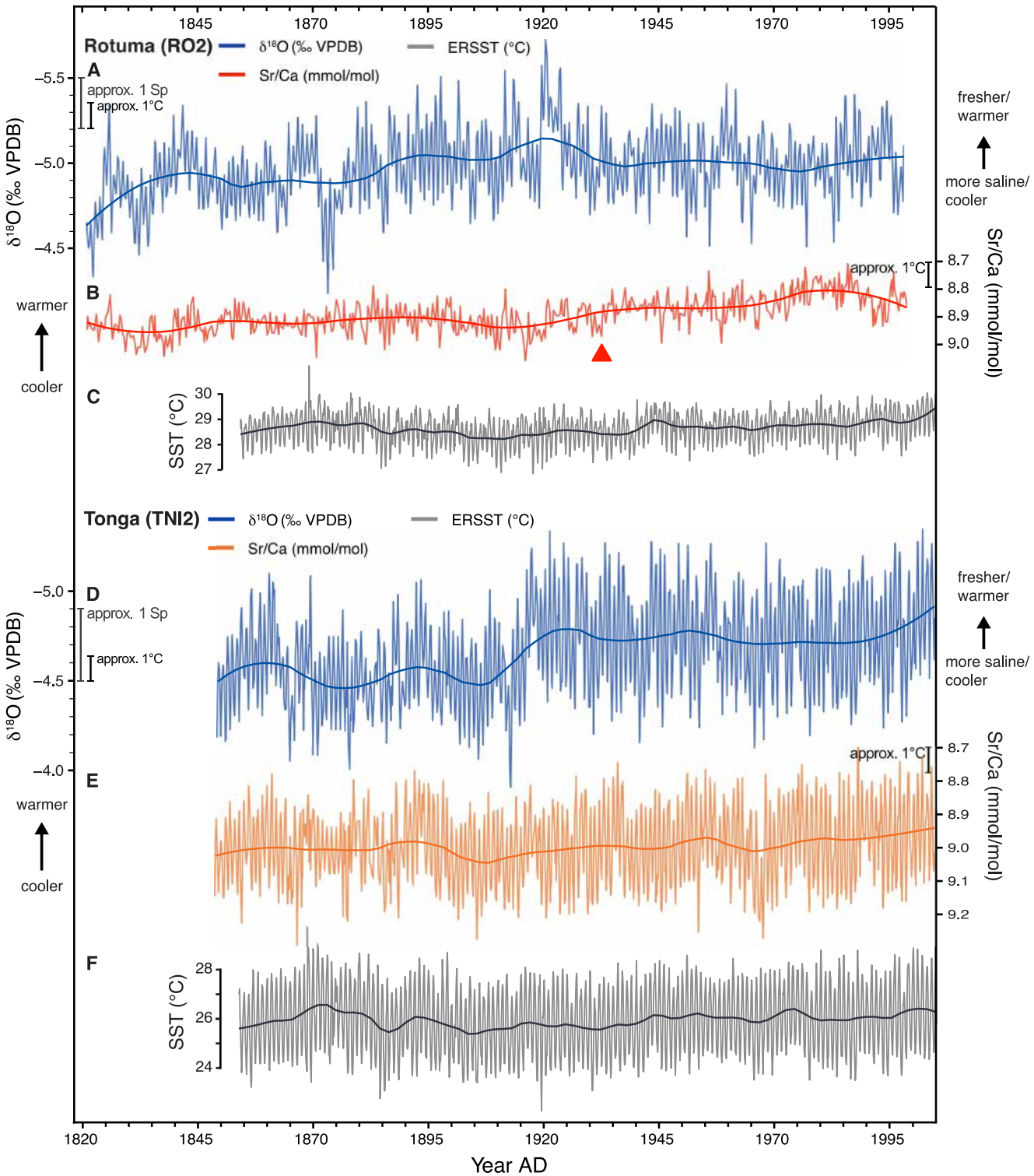

Figure 2. Coral sea surface temperature (SST) proxies in comparison with gridded SST. (a) Rotuma coral monthly $\delta^{18}O$; and (b) Sr/Ca (the red triangle denotes a significant change point in 1933); in comparison to (c) Rotuma ERSST, (d) Tonga monthly $\delta^{18}O$; and (e) Sr/Ca; in comparison to (f) Tonga ERSST. Thicker lines are locally fitted polynomial regressions (LOESS) to emphasize lower frequency variability and secular trends of SST and coral proxies. All records are fitted with bars for an approximate conversion of $\delta^{18}O$ to SST (‰°C^{-1}), and Sr/Ca to SST (mmol mol^{-1}°C^{-1}) based on the slopes obtained and reported in Tables 1 and 2.

Table 3
Secular Trends in Coral Proxies (Spanning the Whole Records) and Change Per Decade Over the 1850–1998 Period

	$\delta^{18}O$ (‰)	Sr/Ca (mmol mol^{-1})	$\delta^{18}O_{sw}$ (‰)
RO2	−0.13	−0.11	0.13
TNI2	−0.36	−0.04	−0.18

Note. All trends are significant at the $p < 0.001$ level.

3.3.2. Sr/Ca

Both corals recorded secular warming trends in Sr/Ca data (Figures 2b and 2e, Table 3). Rotuma Sr/Ca-SST data shows a warming of 1.2 ± 0.08°C, 95% CI in the WPWP during 1850–1998, with a significant change point toward warmer mean values identified in 1933 ($p < 0.0001$). Multiple change points in variance were identified throughout the Rotuma Sr/Ca record (Figure S6, a in Supporting Information S1), the last one coinciding with an anomalously strong cooling in the 1986–1993 period that was not reflected in the instrumental record (Figure 2c). Sr/Ca-SST data from subtropical Tonga shows a lesser degree of warming (0.5 ± 0.02°C, 95% CI) in the same period, and no significant change points in comparison. The seasonal cycles present in the Tonga coral Sr/Ca record reflect local SST conditions and capture the large local SST seasonality (0.27 mmol mol^{-1}, equating to a change of 3.55°C) (Table S3 in Supporting Information S1) while the Rotuma Sr/Ca record did not capture the complete seasonal cycle (0.03 mmol mol^{-1}, equating to a change of 0.30°C) (Table S3 in Supporting Information S1). It should be noted that the standard deviation for each month is higher (0.04–0.05 mmol mol^{-1}) than the seasonal variability range, and annual cycles are quite inconsistent. Annual cycles are periodically not well-defined in Rotuma SST as well, albeit to a smaller extent (Figure S3 in Supporting Information S1).

3.3.3. $\delta^{18}O_{sw}$ Reconstruction

Monthly reconstructed $\delta^{18}O_{sw}$ from coral Sr/Ca and $\delta^{18}O$ values following the method by Ren et al. (2002) is compared to the D-SSS data set (Figure 3). The reconstructed $\delta^{18}O_{sw}$ achieved the highest correlation to this SSS data set, therefore it is our choice for subsequent interpretations. Only data after the year 1960 of the D-SSS were included in the $\delta^{18}O_{sw}$ to SSS calibration for greater reliability due to the decreasing number of observations in preceding years. Interannual and decadal variability is apparent in both corals' data, and more pronounced compared to the annual cycle, similar to the SSS data. An annual cycle is present and has a higher amplitude in Rotuma (0.30‰, 0.50 S_p) compared to Tonga (0.15‰, 0.31 S_p) (Table S3, Supporting Information S1). Similarly, annual cycles in the SSS data in these two locations are also relatively high (0.25 S_p; 0.21 S_p). In the overlapping period (1960–1998), both corals show significant relationships between their $\delta^{18}O_{sw}$ records and SSS data (Figure 3), with Rotuma indicating a higher degree of correlation (Table 2). Both corals exhibit a long-term freshening trend up to around the mid-1910s. However, the freshening trend in Tonga intensifies and a change point toward significantly fresher conditions is identified in the mid-1910s ($p < 0.001$) (Figure S6d, Supporting Information S1), resulting in a significant overall freshening of 0.45 S_p (Table 3). In contrast, the interdecadal shifts between increased salinity and fresher conditions in Rotuma result in an overall insignificant trend. Centered $\delta^{18}O_{sw}$ data from both corals (Figure 3e) reveal a lag in trend shifts from Rotuma in the west to Tonga in the east. The variability of $\delta^{18}O_{sw}$ in Rotuma is also more pronounced than in Tonga, which is characteristic of the fresh WPWP SSS.

3.3.4. $\delta^{18}O$ - A Proxy for SST or SSS

Pseudo-coral $\delta^{18}O$ is a product of modeled coral $\delta^{18}O$ variability from linear bivariate regressions of $\delta^{18}O$ against available instrumental SST and SSS data. Pseudo-coral $\delta^{18}O$ relationship with instrumental SST and SSS can then be used to obtain the relative contributions of temperature and salinity to the $\delta^{18}O$ proxy. Both corals observed $\delta^{18}O$ records correlate strongly with the obtained pseudo-coral $\delta^{18}O$ (Figure 4, A, RO2: $r = 0.70$; Figure 4b, TNI2: $r = 0.84$, $p < 0.001$).

4. Discussion

4.1. Coral $\delta^{18}O$ as a Proxy of SSS in the WPWP

Despite a strong correlation to SST ($r = -0.59$ to -0.68, Table S4, in Supporting Information S1), coral $\delta^{18}O$ values at Rotuma primarily reflect variations of $\delta^{18}O_{sw}$ and SSS as shown by the coral $\delta^{18}O$ forward model results (Figure 4). This aligns with findings from other WPWP corals (Thompson et al., 2022), and reinforces the notion that in the WPWP, coral $\delta^{18}O$ could provide an alternative to $\delta^{18}O_{sw}$-SSS reconstruction where paired Sr/Ca

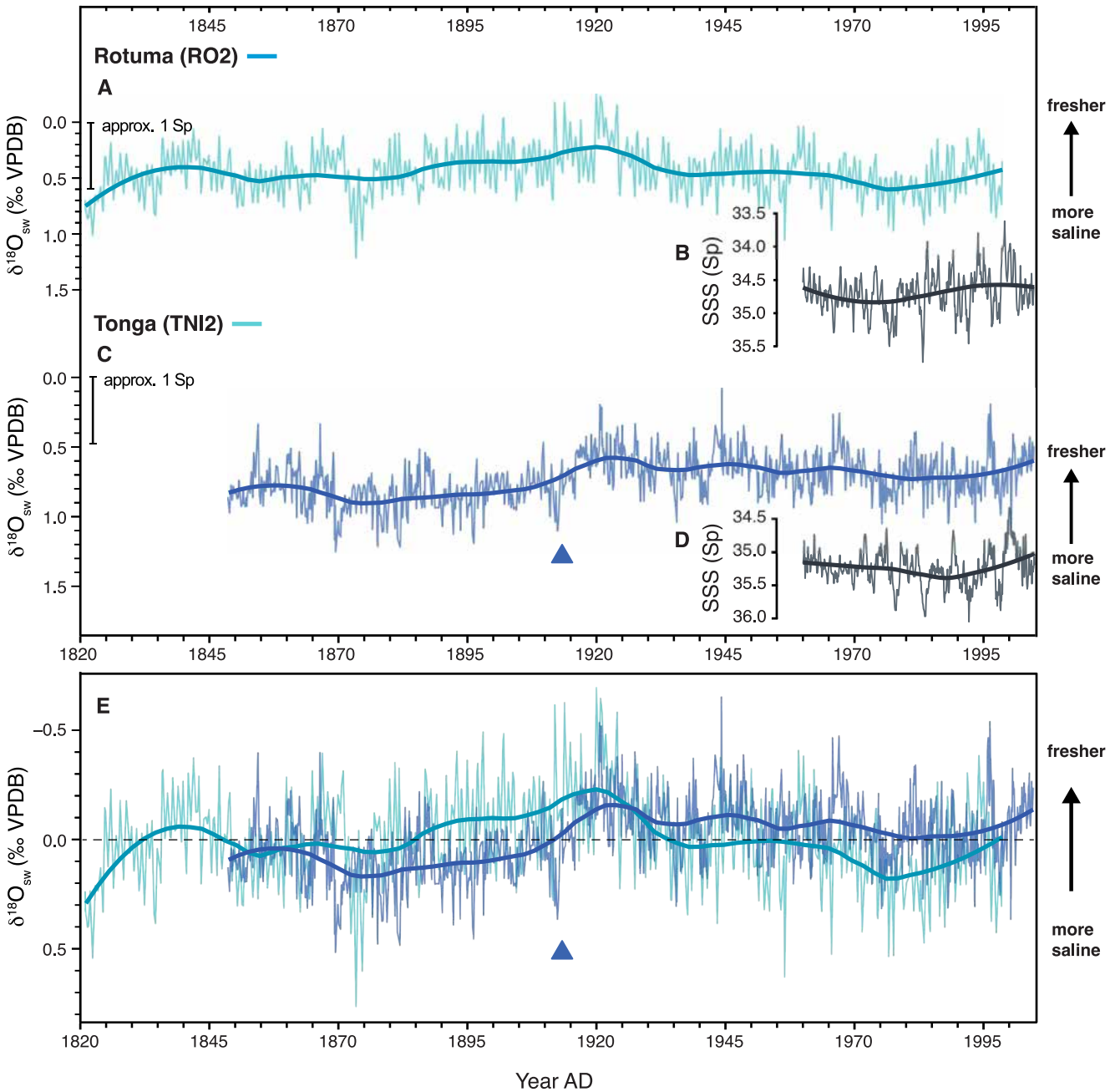

Figure 3. Coral sea surface salinity (SSS) proxy reconstruction in comparison to gridded SSS. (a) Rotuma coral monthly $\delta^{18}O_{sw}$; in comparison to (b) the gridded SSS (D-SSS); (c) Tonga coral monthly reconstructed $\delta^{18}O_{sw}$ (the blue triangle denotes a significant change point in 1914); in comparison to (d) the gridded SSS (D-SSS); (e) The reconstructed monthly $\delta^{18}O_{sw}$ data from Tonga and Rotuma centered by removing their common period mean of 1848–1998 (the blue triangle denotes a significant change point in 1914 in the Tonga time-series). Bold lines are locally fitted polynomial regressions to emphasize the lower frequency variability and secular trends of SSS and coral proxies. Both records are fitted with bars for an approximate conversion of $\delta^{18}O_{sw}$ to SSS (‰ S_p^{-1}), based on the slopes obtained and reported in Tables 1 and 2.

measurements are not available. Thus, $\delta^{18}O$ records can provide vital insights into the past hydroclimate variability of the region where SSS records are short and unreliable. This is further validated by the high proportion of variance ($r^2 = 0.65$) that can be explained between coral $\delta^{18}O$ values and the reconstructed $\delta^{18}O_{sw}$ signature of Rotuma.

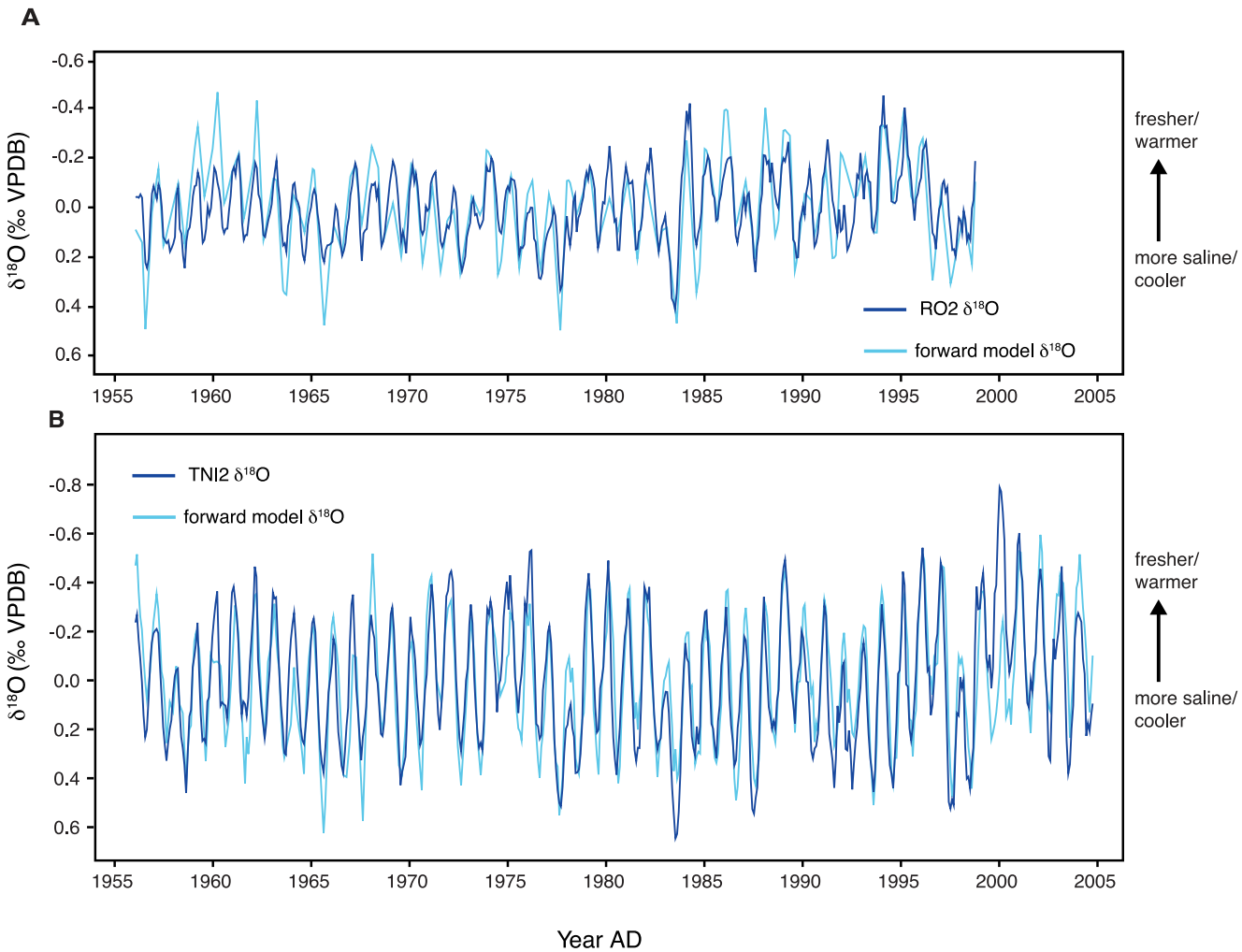

Figure 4. The forward model $\delta^{18}O$ and measured $\delta^{18}O$ with their respective means removed for centering. (a) RO2, (b) TNI2. Pseudo-coral $\delta^{18}O$ indicated different responses of $\delta^{18}O$ to environmental drivers along the South Pacific Convergence Zone axis. Rotuma pseudo-coral $\delta^{18}O$ variability is predominantly driven by sea surface salinity (SSS), while sea surface temperature (SST) is the main driver in Tonga (Table 4). This highlights the importance of proxy choices in SST and SSS reconstructions. Both corals exhibited statistically significant ($p < 0.001$), strong correlations between pseudo-coral $\delta^{18}O$ and coral $\delta^{18}O$, SST, and SSS.

4.2. Coral $\delta^{18}O$ as a Proxy of SST in the Subtropical SW Pacific

Along the SPCZ axis toward Tonga in the southeast, the influence of SST is increasingly reflected in the mean coral $\delta^{18}O$ signature (Figure 2, Linsley et al., 2008). As the coral $\delta^{18}O$ signature becomes more enriched, it reflects predominantly the lower SST of the area on a seasonal timescale, but also drier conditions on an interannual timescale (Linsley et al., 2008), and vice versa. In Tonga, annual coral $\delta^{18}O$ variability is forced predominantly by the SST cycle, similar to other previously published corals from the SPCZ region (Linsley et al., 2006) with the proxy record having a strong relationship to SST, comparable to Sr/Ca-SST obtained here. This is further reinforced by the Tonga pseudocoral $\delta^{18}O$ data reflecting primarily SST variations in the monthly data (Figure 4), as well as Sr/Ca data explaining 62% of the variance in $\delta^{18}O$ data. Nonetheless, the anomalous decrease in $\delta^{18}O$ in 1915 observed in this coral, and not present in the SST data cautions against its use for regional long-term SST reconstruction, as it might have been caused by a tectonic shifting of water depth at this site (Linsley et al., 2008). Since a sizable portion of coral $\delta^{18}O$ values in this subtropical part of the SPCZ region reflects SST trends, paired Sr/Ca data is necessary to remove the SST contribution for the SSS reconstruction (Ren et al., 2002; Weber & Woodhead, 1972). Our results highlight the need for understanding the drivers behind coral $\delta^{18}O$ variability prior to interpretation as an SST or an SSS proxy. This is particularly critical within the SPCZ, where $\delta^{18}O$ variability drivers shift along the constrained gradient extending from the WPWP and following the SPCZ's diagonal axis.

Table 4
Pseudocoral $\delta^{18}O$ Correlations to Coral $\delta^{18}O$, ERSST and D-SSS Data Sets for the Period of 1960–1998

	$\delta^{18}O$- $\delta^{18}O_{pseudo}$, r^2	$\delta^{18}O_{pseudo}$-SST, r^2	$\delta^{18}O_{pseudo}$-SSS, r^2
Rotuma	0.49	0.36	0.77
Tonga	0.71	0.84	0.34

4.3. Sr/Ca-SST Reconstruction

4.3.1. Rotuma

With coral $\delta^{18}O$ variability in Rotuma, being driven primarily by SSS, Sr/Ca is the preferred proxy for SST reconstruction. Rotuma coral Sr/Ca record presented a challenge as it was unable to accurately capture the noisy seasonal variability observed in the SST data sets. Coral Sr/Ca indicated a significant ($p < 0.0001$) but poor correlation with SST over the period 1854–1998, which appears to be likely due to stress response (Figure 5) (Cheung et al., 2021). There were no conclusive observations of physical evidence of stress response visible as stress bands (Figure S1 in Supporting Information S1). The linear extension shows comparable variability between RO2 and TNI2 (Figure S2 in Supporting Information S1) and $\delta^{18}O$ seasonal cycles show consistent cycles. We identified previously reported or reconstructed El Niño (EN), La Niña (LN), and bleaching events (B) (Ray & Giese, 2012; P. Singh et al., 2013; Wolter & Timlin, 2011), and we observed a breakdown of Sr/Ca and SST correlation during these events (e.g. 1937–1945, 1965–1975, 1987 and 1998 EN and B episodes, Figure 5b). Excluding the affected data (763 out of 1738 data points) from the regression improved the relationship significantly ($p < 0.0001$) from $r = -0.21$ to $r = -0.47$. The improved relationship provided a more negative (steeper) OLS regression slope suggesting a stronger SST dependence (Figure S4b in Supporting Information S1), similar to that observed by Cheung et al. (2021). The breakdown in the Sr/Ca-SST relationship has led to significant anti-correlations ($p < 0.05$, Figure 3b, shaded areas) during some (1916–1918 LN, 1941 EN, 1966 EN, 1974 LN, 1987 EN, 1998 EN) but not all events classified as strong/very strong. Similar to the observed impacts of the 1997/98 El Niño/La Niña events in the Red Sea (D'Olivo et al., 2019), we observe disruptions in the normally highly correlated Sr/Ca and SST relationship. These disruptions sometimes carry on over three to five years when stress events are consequent.

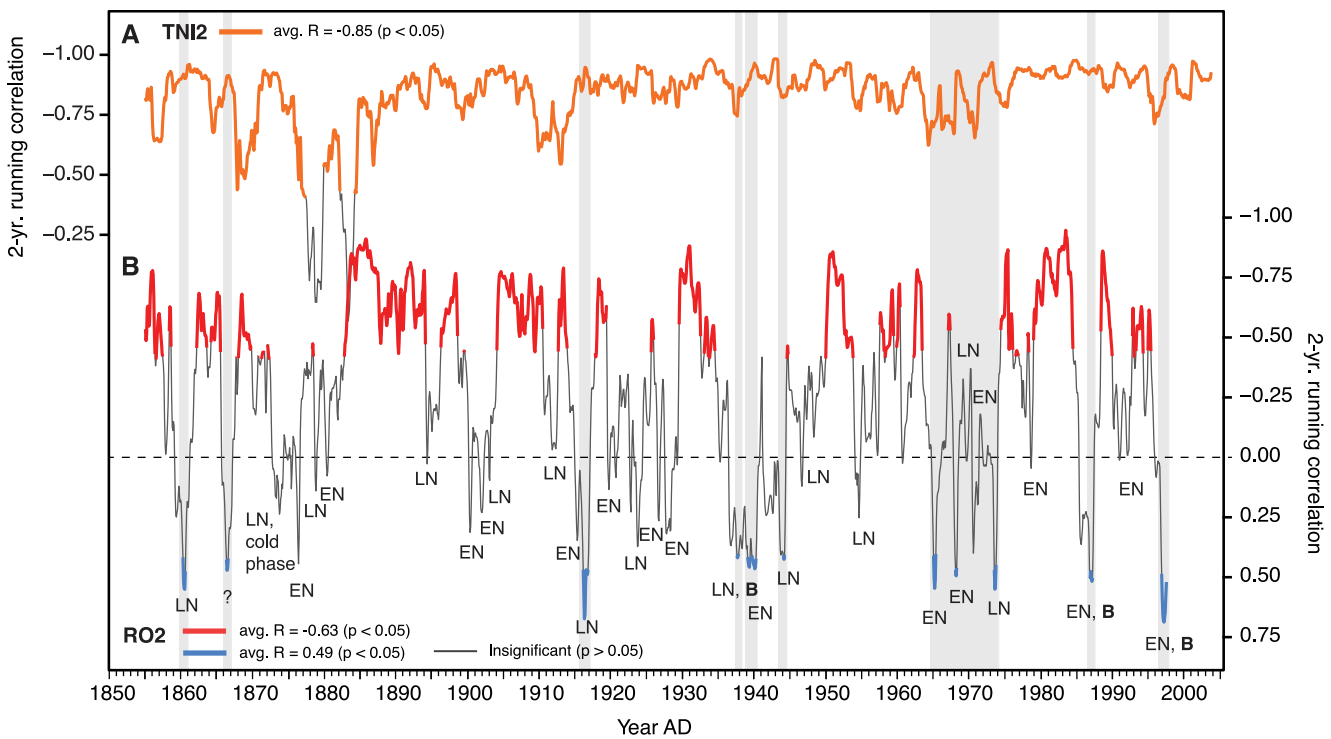

Figure 5. 24-month window moving correlation between monthly coral Sr/Ca and ERSST shows differing responses between the RO2 and TNI2 corals. While simple OLS and Reduced Major Axis calibration regressions show weak relationships between RO2 Sr/Ca and sea surface temperature, rolling correlation shows most data correlates significantly (53%, average $r = -0.63$, $p < 0.05$), albeit with episodes of highly unusual positive correlation indicating breaks in the Sr/Ca-SST relationship atypical in tropical warm water corals (17%, average $r = 0.49$, $p < 0.05$). Most episodes coincide with weaker correlations in the TNI2 coral as well (late 1970s, late 1930s, mid-1960s to mid-1970s). Most of periods of insignificant or significantly positive correlation in RO2 coincide with El Niño (EN) and La Niña (LN) events or recorded bleaching episodes (B).

The reconstructed SST based on the Sr/Ca-SST sensitivity obtained by RMA regression is in closer agreement with the instrumental SST records. The slopes obtained from the regression of the full Sr/Ca data with ERSST, compared to the one where data affected by no significant correlation or anti-correlation were removed, were much steeper than those from OLS regressions and almost identical in both cases (−0.090 and −0.091 mmol $mol^{-1}°C^{-1}$, respectively). Such a relationship has also been documented in a coral from Papua New Guinea with an even steeper Sr/Ca-SST calibration slope of −0.23 mmol $mol^{-1}°C^{-1}$ (Alibert & Kinsley, 2008). Steeper slopes of −0.084 mmol $mol^{-1}°C^{-1}$ have been suggested to achieve a higher fidelity in Sr/Ca-SST calibration due to possible signal attenuation during skeleton precipitation ("bio-smoothing") that can span over a period of up to 1 year (Gagan et al., 2012). Currently, there are limited Sr/Ca-SST reconstructions from the WPWP (Alibert & Kinsley, 2008; Quinn et al., 2006), and most relationships described in the Southwest Pacific are from locations with a higher seasonal SST amplitude (Corrège, 2006, and references therein). Corals accustomed to these conditions are less susceptible to heat stress (Carilli et al., 2012; Oliver & Palumbi, 2011; Safaie et al., 2018) and show more typical Sr/Ca-SST relationships with slopes ranging from −0.05 to −0.07 mmol per °C for the seasonal SST amplitudes above 3°C (e.g., Gagan et al., 1998; Linsley et al., 2000; Marshall & McCulloch, 2002; Quinn & Sampson, 2002; Wu et al., 2013), similar to our observation in Tonga.

Rotuma is located in an area of persistent high convergence and cloudiness, undergoing a complicated annual precipitation cycle making for a challenging case in representing the regional SST conditions with its reef-scale variability. After the main SST peak in January/February, a dip in SST occurs due to high precipitation most commonly in February/March, after which the SST increases again, producing another peak in March/April (Reynolds et al., 2002). An additional challenge posed in this region is the fact that the SST products available are based on limited historical observations. In addition to the lack of in-situ SST measurements that overlap with the coral proxy record, it also cannot be excluded that the coral Sr/Ca values may be recording local conditions of the bay where it was collected. As shown by the SST data set comparisons (see Table S2 in Supporting Information S1), there is less variability explained between different data sets in Rotuma compared to Tonga, making the instrumental SST for this location less reliable even on the regional scale. These limitations hamper the application of the Rotuma coral Sr/Ca record to represent highly resolved regional scale SST. However, no impact on the Sr/Ca-SST RMA regression slope when stress-affected data are removed concurrent with a significant increase in correlation shows that the longer-term secular trends as well as environmental stress are recorded in the coral Sr/Ca values (Figure 5, Figure S4 in Supporting Information S1).

4.3.2. Tonga

The Tonga coral shows an impressive correlation between skeletal $\delta^{18}O$ signature, Sr/Ca values, and instrumental SST data (Figures 2d–2f). Monthly-resolved proxy data captures the seasonal cycle and can be used for highly resolved reconstructions. The rolling correlation of 2 years suggests there are periods of lower correlation and a breakdown in the coral Sr/Ca-SST relationship in the mid-1870s to mid-1880s (Figure 5a). This result may be an artifact of the SST observations contributing to the ERSST data set in this period and be indicative of stress events by the coral itself. Overall, Tonga coral Sr/Ca record presented in this study is an excellent complement to the published records from Fiji and Rarotonga for reconstructions of oceanographic variability gradients along the SPCZ axis (Linsley et al., 2000, 2004). Moreover, this record complements the previously published record from Tonga (Wu et al., 2013) as a higher resolved replication record for the extension of the reconstructed temporal SST variability.

4.4. SST Trends Along the SPCZ Axis

ERSST shows similar rates of warming in both Tonga and Rotuma, with visible decadal timescale variability. The warming trend of the SPCZ has been consistent and steady since the 1900s, resulting in a 0.60°C increase in Rotuma, and a 0.72°C increase in Tonga until the end of each coral record (Table 5). Both corals exhibit clear secular negative trends in the monthly-resolved Sr/Ca data (Figures 2b and 2e, Table 3) and suggest warming since the late 1800s-early 1900s, with a significant change point in early 1933 ($p < 0.001$) in Rotuma, indicating a significant shift in mean values toward warmer temperatures (Figure S6 in Supporting Information S1). The total warming in the WPWP coral data shows approximately 1.5°C warming since 1900 and around 1°C in the subtropical Tonga coral (Figures 2c and 2f, Table 5). Similar rates of warming have been reported from other corals in the SPCZ as well with Wu et al. (2013) reporting 1.2°C warming in Fiji and 1.8°C in Tonga since 1900. WPWP adjacent *Porites* sp. from Timor shows a 1.7°C warming in the twentieth century in its Sr/Ca record (Cahyarini

Table 5
Warming Trends Estimated From Coral Proxies and Instrumental Data Since 1900 and Salinity Trends Since 1950

	Proxy (95% CI)	Change since 1900°C/S_p	Change since 1950°C/S_p
RO2 Sr/Ca	−0.09 mmol/mol per °C (−0.095, −0.084)	**+1.53 ± 0.10°C**	**+0.60 ± 0.04°C**
ERSST (Rotuma)		**+0.60°C**	**+0.25°C**
RO2 $\delta^{18}O_{sw}$	0.60‰ per S_p (0.55, 0.64)		***0.105 ± 0.005*** S_p
D-SSS (Rotuma)			***−0.10*** S_p
TNI2 Sr/Ca	−0.083 mmol/mol per °C (−0.086, −0.080)	**+0.95 ± 0.04°C**	**+0.40 ± 0.02°C**
ERSST (Tonga)		**+0.74°C**	**+0.13°C**
TNI2 $\delta^{18}O_{sw}$	0.47‰ per S_p (0.43, 0.51)		*−0.03* S_p
D-SSS (Tonga)			*−0.02* S_p

Note. Significant at $p < 0.0001$ in bold, $p < 0.05$ in bold italic, insignificant in italic. Coral proxy long-term change is calculated by dividing the trend by proxy 95% bootstrapped CI to obtain the possible range of change.

et al., 2014). Our results suggest there has been disproportionately more warming in the WPWP region than shown by gridded SST products (Cravatte et al., 2009). Climate model simulations observing the trend since the 1950s show only a 0.3°C increase in the WPWP (Weller et al., 2016), but there is a discussion on how reliable model outputs and gridded data are in this region (van Hooidonk & Huber, 2009; Vecchi et al., 2008). Gridded SST products used in Sr/Ca-SST calibrations average data at coarse spatial resolutions, possibly escaping the local influences of oceanographic and mesoscale atmospheric processes on SST, misrepresenting the near-shore warming. Models such as CMIP5 and CMIP6 struggle in constraining tropical SST gradients and underestimate the warming in the WPWP compared to the one observed in instrumental data over the past few decades (Bai et al., 2022, 2024; Leung et al., 2022; X. Liu & Grise, 2023) (Figure S5 in Supporting Information S1). Our findings from Rotuma and Tonga support observed WPWP extension since 1900 and intensification since the 1980s (Roxy et al., 2019). While gridded and reanalysis SST data is the best available data in this region, it is worth noting that these data sets are produced from sparse observations over large spatial scales. Missing values are interpolated and only provide the best estimate in lieu of real values (Huang et al., 2015; Kennedy et al., 2011a, 2011b; Rayner et al., 2003; Yasunaka & Hanawa, 2011).

4.5. SPCZ Hydroclimate Reconstruction

Different instrumental SSS data sets show very little similarity between each other for the same location, highlighting how unreliable these data sets are in describing Southwest Pacific SSS variability. We find that even the data set best correlated to coral $\delta^{18}O_{sw}$, D-SSS, often smooths out the approximate 0.7–0.9 S_p of annual variability seen in Tonga in the calibration period (Figure 3). RMA regression is an especially better choice for $\delta^{18}O_{sw}$ -SSS calibration compared to OLS as it minimizes residuals for both variables, thus increasing the robustness of resulting estimates (Nurhati et al., 2011; Solow & Huppert, 2004). We find that slopes obtained in our calibrations are much higher than the conservative slopes of 0.14–0.36‰ S_p^{-1} previously established from $\delta^{18}O_{sw}$-SSS *Porites* sp. reconstructions in the Western Pacific (Fairbanks et al., 1997; Kilbourne et al., 2004; Linsley et al., 2006; Wu et al., 2013).

Regarding the trends in the coral records and instrumental SSS data sets since 1950, both coral and instrumental data agree on the lack of significant trends in Tonga (Table 5). In Rotuma, even though instrumental SSS data shows a freshening of 0.10 S_p since 1950, the coral shows an opposite trend. This contrasts with previous findings from instrumental SSS reanalysis that found an overall decrease of 0.20 S_p in the South Pacific since 1950 (Cravatte et al., 2009). Delcroix et al. (2007) found a decrease of 0.10–0.20 S_p since the 1970s in the Southwest Pacific, based on ship track SSS measurements, but the data doesn't cover Rotuma. As seen in Figure 3 though, while the Rotuma $\delta^{18}O_{sw}$ record doesn't show a significant secular trend, the Tonga coral $\delta^{18}O_{sw}$ record shows significant long-term freshening of 0.45 S S_p *Porites* sp.-based reconstructions from Fiji and Tonga reported by Wu et al. (2013) show a centennial trend of −0.17 to −0.22 S_p in comparison, which is obtained by using a 0.19‰ S_p^{-1} slope that might influence the difference in magnitude compared to our results. Central Pacific reconstruction from Palmyra *Porites* sp. reports a century-long trend of −0.90 S_p using the Fairbanks et al. (1997) empirical $\delta^{18}O_{sw}$-SSS relationship of 0.27‰ S_p^{-1} (Nurhati et al., 2011). Observed freshening since the mid-

1910s in Tonga supports the previous findings of southeastward expansion of the salinity front since the beginning of the twentieth century (Dassié et al., 2018; Nurhati et al., 2011; Wu et al., 2013). The reasons for this expansion neither seem to be due to increased rainfall (Dassié et al., 2018), despite the global coupled model predictions inferences of increased precipitation in convective regions (Xie et al., 2010), nor a long-term shift in SPCZ position in the past century (Salinger et al., 2014). Recent work highlights the influence of wind stress on surface salinity changes on decadal timescales (Li et al., 2019), as well as on ocean circulation patterns (Chen et al., 2023; Heede & Fedorov, 2023; L'Heureux et al., 2013), due to current transport relaxing or strengthening. Expansion of the fresh pool observed by the displacement of the salinity front indicates a shift toward a La Niña-like climate state where enhanced convection and warming are driving more extreme precipitation events which agrees with observational precipitation data in the SPCZ (Griffiths et al., 2003). This expansion is concurrent with the WPWP expansion and differentially higher rates of warming in the tropical Western Pacific due to rising CO_2 forcing (Peter et al., 2023; Roxy et al., 2019; Seager et al., 2019). With enhanced shallow subtropical-tropical cells overturning, and saltier subtropical waters being subducted into the tropics, the lower-salinity waters of the fresh pool would expand into the subtropics driving freshening trends in Tonga.

4.6. Summary

Two new monthly-resolved coral Sr/Ca records and $\delta^{18}O_{sw}$ reconstructions from Rotuma and Tonga demonstrate the temporal evolution and spatial variability of SST and SSS in the WPWP and SPCZ regions. We establish that the coral $\delta^{18}O$ signature is principally an SSS proxy in the WPWP. Therefore, additional coral-based SST proxies should be employed for reconstructions in the WPWP. Discrepancies between WPWP observed SSTs and reconstructed coral-based SSTs can be due to coral physiological stress response affecting seasonal cyclicity (D'Olivo et al., 2019; Marshall & McCulloch, 2002), growth-related signal attenuation (Gagan et al., 2012), the coral recording more local SST rather than regional. Periods of ENSO positive and negative phases, and bleaching events coincide with Sr/Ca-SST relationship breaks. Nonetheless, we show that the calibration regressions can be improved with the identification and removal of periods of stress to the coral. Although high-resolution, monthly SST reconstruction from Rotuma may be inaccurate due to disruptions to the Sr/Ca-SST relationship, the secular trend from this coral remains unaffected. This is evident as the regression of data unaffected by these disruptions yields the same slope and intercept as the full data set, while significantly improving the correlation between Sr/Ca and SST. Steeper slopes achieved with the RMA regression correspond well with the growth-corrected slopes suggested by Gagan et al. (2012) for estimating twentieth century trends. While both corals show a warming trend, our results suggest a higher degree of warming and an earlier onset in the WPWP than described by available instrumental data. Another major implication of our study is in confirming the long-term trend of the eastward displacement of the SPCZ since the early 1900s. At the same time, our records establish that there are no pronounced long-term changes in salinity in the WPWP.

The new coral Sr/Ca-SST records enable a greater understanding of local and regional processes in the SPCZ and suggest that further replication is necessary for a more suitable representation of the WPWP. The two new coral records from Tonga and Rotuma presented here add to the existing network of previously published SPCZ coral records which could pave the way to better proxy-based reconstructions with multi-coral reconstructions spanning over a larger area in the Southwest Pacific. Additional coral records will improve the signal-to-noise ratio for higher fidelity reconstructions of the SPCZ longer-term, interannual, and interdecadal variability.

Conflict of Interest

The authors declare no conflicts of interest relevant to this study.

Data Availability Statement

Open Access funding enabled and organized by Projekt DEAL. All data reported in this study have been deposited at the PANGAEA Repository (Data Publisher for Earth and Environmental Science), at Todorovic et al. (2024). R statistical software was used for statistical and data analyses (R Core Team, 2021). The ERSST data set (Huang et al., 2015) is publicly available and was obtained from the IRI/LDEO Climate Data Library (http://iridl.ldeo.columbia.edu/SOURCES/.NOAA/.NCDC/.ERSST/index.html, accessed 28 May 2020). OISSTv2.1 is also publicly available (Reynolds et al., 2002) and was retrieved from the IRI/LDEO Climate Data Library (http://iridl.ldeo.columbia.edu/SOURCES/.NOAA/.NCEP/.EMC/.CMB/.GLOBAL/.Reyn_SmithOIv2/.

monthly/index.html, accessed 28 May 2020). D-OISSTv2.1 (Huang et al., 2021) is publicly available and was retrieved from the NOAA PSL library (https://psl.noaa.gov/data/gridded/data.noaa.oisst.v2.highres.html, accessed 2 February 2022). The SODA SSS v2.2.4 (Carton & Giese, 2008) data set was accessed through the ERDDAP NOAA data library, and is publicly available (https://coastwatch.pfeg.noaa.gov/erddap/griddap/hawaii_d90f_20ee_c4cb.html, accessed 05 April 2024). The Delcroix SSS Product (Delcroix et al., 2011) is publicly available through the Sedoo repository (https://sss.sedoo.fr/landing-page/?uuid=3b107323-0fde-067e-1ba2-f819f2900f50 accessed 1 August 2022). ORA-20C SST and SSS products (de Boisséson et al., 2018) are available through the University of Hamburg repository (https://www.cen.uni-hamburg.de/en/icdc/data/ocean/easy-init-ocean/ecmwf-ensemble-of-ocean-reanalyses-of-the-20th-century-ora-20c.html), but were obtained privately from Christophe Menkes on 5 October 2023.

Acknowledgments
We thank Sebastian Flotow and Jule Mawick for their generous laboratory assistance with coral core slabbing and ICP-MS analysis. We thank Sharon Dbritto and Sahra Greve for their assistance with coral sampling and laboratory support. We thank Marie Harbott for her constructive comments on the manuscript. We would also like to thank Franz Lehmann, Application Specialist of Analytik Jena GmbH for the excellent customer service in troubleshooting and technical support for our ICP-MS. Dr. med. Ralf Windmann and his team at the Zentrum für Moderne Diagnostik (ZEMODI, Bremen, Germany) generously helped with coral X-radiograph imaging free of charge. Major funding for this work was provided to HCW. The OASIS project was funded by the Federal Ministry of Education and Research (BMBF) under the "Make Our Planet Great Again – German Research Initiative," Grant 57429626 to Dr. Henry C. Wu (Junior Research Group Leader), implemented by the German Academic Exchange Service (DAAD). Open Access funding enabled and organized by Projekt DEAL.

References

Alibert, C., & Kinsley, L. (2008). A 170-year Sr/Ca and Ba/Ca coral record from the western Pacific warm pool: 1. What can we learn from an unusual coral record? *Journal of Geophysical Research*, *113*(C4), C04008. https://doi.org/10.1029/2006JC003979

Alibert, C., & McCulloch, M. T. (1997). Strontium/calcium ratios in modern *Porites* corals from the Great Barrier Reef as a proxy for sea surface temperature: Calibration of the thermometer and monitoring of ENSO. *Paleoceanography*, *12*(3), 345–363. https://doi.org/10.1029/97PA00318

Alpert, A. E., Cohen, A. L., Oppo, D. W., DeCarlo, T. M., Gove, J. M., & Young, C. W. (2016). Comparison of equatorial Pacific sea surface temperature variability and trends with Sr/Ca records from multiple corals. *Paleoceanography*, *31*(2), 252–265. https://doi.org/10.1002/2015PA002897

Bagnato, S., Linsley, B. K., Howe, S. S., Wellington, G. M., & Salinger, J. (2005). Coral oxygen isotope records of interdecadal climate variations in the South Pacific Convergence Zone region. *Geochemistry, Geophysics, Geosystems*, *6*(6). https://doi.org/10.1029/2004GC000879

Bai, W., Liu, H., Lin, P., Hu, S., & Wang, F. (2022). Indo-Pacific warm pool present warming attribution and future projection constraint. *Environmental Research Letters*, *17*(5), 054026. https://doi.org/10.1088/1748-9326/ac5edf

Bai, W., Liu, H., Lin, P., & Shen, H. (2024). The simulation of the Indo-Pacific warm pool SST warming trend in CMIP5 and CMIP6. *Geoscience Letters*, *11*(1), 31. https://doi.org/10.1186/s40562-024-00346-6

Beaulieu, C., & Killick, R. (2018). Distinguishing trends and shifts from memory in climate data. *Journal of Climate*, *31*(23), 9519–9543. https://doi.org/10.1175/JCLI-D-17-0863.1

Brown, J. R., Lengaigne, M., Lintner, B. R., Widlansky, M. J., van der Wiel, K., Dutheil, C., et al. (2020). South Pacific Convergence Zone dynamics, variability and impacts in a changing climate. *Nature Reviews Earth & Environment*, *1*(10), 530–543. https://doi.org/10.1038/s43017-020-0078-2

Cahyarini, S. Y., Pfeiffer, M., & Dullo, W.-C. (2009). Improving SST reconstructions from coral Sr/Ca records: Multiple corals from Tahiti (French Polynesia). *International Journal of Earth Sciences*, *98*(1), 31–40. https://doi.org/10.1007/s00531-008-0323-2

Cahyarini, S. Y., Pfeiffer, M., Nurhati, I. S., Aldrian, E., Dullo, W.-C., & Hetzinger, S. (2014). Twentieth century sea surface temperature and salinity variations at Timor inferred from paired coral $\delta^{18}O$ and Sr/Ca measurements. *Journal of Geophysical Research: Oceans*, *119*(7), 4593–4604. https://doi.org/10.1002/2013JC009594

Cahyarini, S. Y., Pfeiffer, M., Timm, O., Dullo, W.-C., & Schönberg, D. G. (2008). Reconstructing seawater $\delta^{18}O$ from paired coral $\delta^{18}O$ and Sr/Ca ratios: Methods, error analysis and problems, with examples from Tahiti (French Polynesia) and Timor (Indonesia). *Geochimica et Cosmochimica Acta*, *72*(12), 2841–2853. https://doi.org/10.1016/j.gca.2008.04.005

Carilli, J., Donner, S. D., & Hartmann, A. C. (2012). Historical temperature variability affects coral response to heat stress. *PLoS One*, *7*(3), e34418. https://doi.org/10.1371/journal.pone.0034418

Carton, J. A., & Giese, B. S. (2008). A reanalysis of ocean climate using Simple Ocean Data Assimilation (SODA). *Monthly Weather Review*, *136*(8), 2999–3017. https://doi.org/10.1175/2007MWR1978.1

Chen, W.-H., Ren, H., Chiang, J. C. H., Wang, Y.-L., Cai-Li, R.-Y., Chen, Y.-C., et al. (2023). Increased tropical South Pacific western boundary current transport over the past century. *Nature Geoscience*, *16*(7), 590–596. Article 7. https://doi.org/10.1038/s41561-023-01212-4

Cheung, A. H., Cole, J. E., Thompson, D. M., Vetter, L., Jimenez, G., & Tudhope, A. W. (2021). Fidelity of the coral Sr/Ca paleothermometer following heat stress in the northern Galápagos. *Paleoceanography and Paleoclimatology*, *36*(12), e2021PA004323. https://doi.org/10.1029/2021PA004323

Chongyin, L., Mingquan, M., & Guangqing, Z. (1999). The variation of warm pool in the equatorial western Pacific and its impacts on climate. *Advances in Atmospheric Sciences*, *16*(3), 378–394. https://doi.org/10.1007/s00376-999-0017-0

Clarke, H., D'Olivo, J. P., Conde, M., Evans, R. D., & McCulloch, M. T. (2019). Coral records of variable stress impacts and possible acclimatization to recent marine heat wave events on the northwest shelf of Australia. *Paleoceanography and Paleoclimatology*, *34*(11), 1672–1688. https://doi.org/10.1029/2018PA003509

Corrège, T. (2006). Sea surface temperature and salinity reconstruction from coral geochemical tracers. *Palaeogeography, Palaeoclimatology, Palaeoecology*, *232*(2–4), 408–428. https://doi.org/10.1016/j.palaeo.2005.10.014

Cravatte, S., Delcroix, T., Zhang, D., McPhaden, M., & Leloup, J. (2009). Observed freshening and warming of the western Pacific warm pool. *Climate Dynamics*, *33*(4), 565–589. https://doi.org/10.1007/s00382-009-0526-7

D'Arrigo, R., Wilson, R., Palmer, J., Krusic, P., Curtis, A., Sakulich, J., et al. (2006). The reconstructed Indonesian warm pool sea surface temperatures from tree rings and corals: Linkages to Asian monsoon drought and El Niño–Southern Oscillation. *Paleoceanography*, *21*(3). https://doi.org/10.1029/2005PA001256

Dassié, E. P., Hasson, A., Khodri, M., Lebas, N., & Linsley, B. K. (2018). Spatiotemporal variability of the South Pacific Convergence Zone fresh pool eastern front from coral-derived surface salinity data. *Journal of Climate*, *31*(8), 3265–3288. https://doi.org/10.1175/JCLI-D-17-0071.1

Dassié, E. P., Linsley, B. K., Corrège, T., Wu, H. C., Lemley, G. M., Howe, S., & Cabioch, G. (2014). A Fiji multi-coral $\delta^{18}O$ composite approach to obtaining a more accurate reconstruction of the last two-centuries of the ocean-climate variability in the South Pacific Convergence Zone region. *Paleoceanography*, *29*(12), 1196–1213. https://doi.org/10.1002/2013PA002591

de Boisséson, E., Balmaseda, M. A., & Mayer, M. (2018). Ocean heat content variability in an ensemble of twentieth century ocean reanalyses. *Climate Dynamics*, *50*(9), 3783–3798. https://doi.org/10.1007/s00382-017-3845-0

DeCarlo, T. M., & Cohen, A. L. (2017). Dissepiments, density bands and signatures of thermal stress in *Porites* skeletons. *Coral Reefs*, *36*(3), 749–761. https://doi.org/10.1007/s00338-017-1566-9

DeCarlo, T. M., Gaetani, G. A., Holcomb, M., & Cohen, A. L. (2015). Experimental determination of factors controlling U/Ca of aragonite precipitated from seawater: Implications for interpreting coral skeleton. *Geochimica et Cosmochimica Acta*, *162*, 151–165. https://doi.org/10.1016/j.gca.2015.04.016

Delcroix, T., Alory, G., Cravatte, S., Corrège, T., & McPhaden, M. J. (2011). A gridded sea surface salinity data set for the tropical Pacific with sample applications (1950–2008). *Deep Sea Research Part I: Oceanographic Research Papers*, *58*(1), 38–48. https://doi.org/10.1016/j.dsr.2010.11.002

Delcroix, T., Cravatte, S., & McPhaden, M. J. (2007). Decadal variations and trends in tropical Pacific sea surface salinity since 1970. *Journal of Geophysical Research*, *112*(C3). https://doi.org/10.1029/2006JC003801

de Villiers, S., Shen, G. T., & Nelson, B. K. (1994). The Sr/Ca-temperature relationship in coralline aragonite: Influence of variability in $(Sr/Ca)_{seawater}$ and skeletal growth parameters. *Geochimica et Cosmochimica Acta*, *58*(1), 197–208. https://doi.org/10.1016/0016-7037(94)90457-X

D'Olivo, J. P., Georgiou, L., Falter, J., DeCarlo, T. M., Irigoien, X., Voolstra, C. R., et al. (2019). Long-term impacts of the 1997–1998 bleaching event on the growth and resilience of massive *Porites* corals from the central Red Sea. *Geochemistry, Geophysics, Geosystems*, *20*(6), 2936–2954. https://doi.org/10.1029/2019GC008312

Dutheil, C., Lengaigne, M., Vialard, J., Jullien, S., & Menkes, C. (2022). Western and central tropical Pacific rainfall response to climate change: Sensitivity to projected sea surface temperature patterns. *Journal of Climate*, *35*(18), 6175–6189. https://doi.org/10.1175/JCLI-D-22-0062.1

Fairbanks, R. G., Evans, M. N., Rubenstone, J. L., Mortlock, R. A., Broad, K., Moore, M. D., & Charles, C. D. (1997). Evaluating climate indices and their geochemical proxies measured in corals. *Coral Reefs*, *16*(1), S93–S100. https://doi.org/10.1007/s003380050245

Folland, C. K., Renwick, J. A., Salinger, M. J., & Mullan, A. B. (2002). Relative influences of the interdecadal Pacific oscillation and ENSO on the South Pacific Convergence Zone. *Geophysical Research Letters*, *29*(13). 21-1. https://doi.org/10.1029/2001GL014201

Gaetani, G. A., & Cohen, A. L. (2006). Element partitioning during precipitation of aragonite from seawater: A framework for understanding paleoproxies. *Geochimica et Cosmochimica Acta*, *70*(18), 4617–4634. https://doi.org/10.1016/j.gca.2006.07.008

Gagan, M. K., Ayliffe, L. K., Hopley, D., Cali, J. A., Mortimer, G., Chappell, J., et al. (1998). Temperature and surface-ocean water balance of the mid-Holocene tropical western Pacific. *Science*, *279*(5353), 1014–1018. https://doi.org/10.1126/science.279.5353.1014

Gagan, M. K., Dunbar, G. B., & Suzuki, A. (2012). The effect of skeletal mass accumulation in *Porites* on coral Sr/Ca and $\delta^{18}O$ paleothermometry. *Paleoceanography*, *27*(1). https://doi.org/10.1029/2011pa002215

Gouriou, Y., & Delcroix, T. (2002). Seasonal and ENSO variations of sea surface salinity and temperature in the South Pacific Convergence Zone during 1976-2000. *Journal of Geophysical Research*, *107*(C12). SRF 12-1-SRF 12-14. https://doi.org/10.1029/2001JC000830

Greene, J. S., Klatt, M., Morrissey, M., & Postawko, S. (2008). The comprehensive Pacific rainfall database. *Journal of Atmospheric and Oceanic Technology*, *25*(1), 71–82. https://doi.org/10.1175/2007JTECHA904.1

Griffiths, G. M., Salinger, M. J., & Leleu, I. (2003). Trends in extreme daily rainfall across the South Pacific and relationship to the South Pacific Convergence Zone. *International Journal of Climatology*, *23*(8), 847–869. https://doi.org/10.1002/joc.923

Hathorne, E. C., Gagnon, A., Felis, T., Adkins, J., Asami, R., Boer, W., et al. (2013). Interlaboratory study for coral Sr/Ca and other element/Ca ratio measurements. *Geochemistry, Geophysics, Geosystems*, *14*(9), 3730–3750. https://doi.org/10.1002/ggge.20230

Heede, U. K., Fedorov, A., & Burls, N. (2021). A stronger versus weaker Walker: Understanding model differences in fast and slow tropical Pacific responses to global warming. *Climate Dynamics*, *57*(9–10), 2505–2522. https://doi.org/10.1007/s00382-021-05818-5

Heede, U. K., & Fedorov, A. V. (2023). Colder eastern equatorial Pacific and stronger walker circulation in the early 21st century: Separating the forced response to global warming from natural variability. *Geophysical Research Letters*, *50*(3), e2022GL101020. https://doi.org/10.1029/2022GL101020

Howell, P., Pisias, N., Ballance, J., Baughman, J., & Ochs, L. (2006). *ARAND time-series analysis software* (p. 685). Brown University.

Huang, B., Banzon, V., Freeman, J., Lawrimore, J., Liu, W., Peterson, T., et al. (2015). Extended reconstructed sea surface temperature version 4 (ERSST.v4). Part I: Upgrades and intercomparisons. *Journal of Climate*, *28*(3), 911–930. https://doi.org/10.1175/JCLI-D-14-00006.1

Huang, B., Liu, C., Banzon, V., Freeman, E., Graham, G., Hankins, B., et al. (2021). Improvements of the daily Optimum interpolation sea surface temperature (DOISST) version 2.1. *Journal of Climate*, *34*(8), 2923–2939. https://doi.org/10.1175/JCLI-D-20-0166.1

Inoue, M., Gussone, N., Koga, Y., Iwase, A., Suzuki, A., Sakai, K., & Kawahata, H. (2015). Controlling factors of Ca isotope fractionation in scleractinian corals evaluated by temperature, pH and light controlled culture experiments. *Geochimica et Cosmochimica Acta*, *167*, 80–92. https://doi.org/10.1016/j.gca.2015.06.009

Juillet-Leclerc, A., Thiria, S., Naveau, P., Delcroix, T., Le Bec, N., Blamart, D., & Corrège, T. (2006). SPCZ migration and ENSO events during the 20th century as revealed by climate proxies from a Fiji coral. *Geophysical Research Letters*, *33*(17), L17710. https://doi.org/10.1029/2006GL025950

Kennedy, J. J., Rayner, N. A., Smith, R. O., Parker, D. E., & Saunby, M. (2011a). Reassessing biases and other uncertainties in sea surface temperature observations measured in situ since 1850: 1. Measurement and sampling uncertainties. *Journal of Geophysical Research*, *116*(D14), D14103. https://doi.org/10.1029/2010JD015218

Kennedy, J. J., Rayner, N. A., Smith, R. O., Parker, D. E., & Saunby, M. (2011b). Reassessing biases and other uncertainties in sea surface temperature observations measured in situ since 1850: 2. Biases and homogenization. *Journal of Geophysical Research*, *116*(D14), D14104. https://doi.org/10.1029/2010JD015220

Kilbourne, K. H., Quinn, T. M., Taylor, F. W., Delcroix, T., & Gouriou, Y. (2004). El Niño–Southern Oscillation–related salinity variations recorded in the skeletal geochemistry of a *Porites* coral from Espiritu Santo, Vanuatu. *Paleoceanography*, *19*(4), 1–8. https://doi.org/10.1029/2004pa001033

Killick, R., & Eckley, I. A. (2014). changepoint: An *R* package for changepoint analysis. *Journal of Statistical Software*, *58*(3). https://doi.org/10.18637/jss.v058.i03

Kuleshov, Y., McGree, S., Jones, D., Charles, A., Cottrill, A., Prakash, B., et al. (2014). Extreme weather and climate events and their impacts on island countries in the western Pacific: Cyclones, floods and droughts. *Atmospheric and Climate Sciences*, *4*(5), 803–818. Article 5. https://doi.org/10.4236/acs.2014.45071

Le Bec, N., Julliet-Leclerc, A., Corrège, T., Blamart, D., & Delcroix, T. (2000). A coral $\delta^{18}O$ record of ENSO driven sea surface salinity variability in Fiji (south-western tropical Pacific). *Geophysical Research Letters*, *27*(23), 3897–3900. https://doi.org/10.1029/2000gl011843

Lebrato, M., Garbe-Schönberg, D., Müller, M. N., Blanco-Ameijeiras, S., Feely, R. A., Lorenzoni, L., et al. (2020). Global variability in seawater Mg:Ca and Sr:Ca ratios in the modern ocean. *Proceedings of the National Academy of Sciences*, *117*(36), 22281–22292. https://doi.org/10.1073/pnas.1918943117

LeGrande, A. N., & Schmidt, G. A. (2006). Global gridded data set of the oxygen isotopic composition in seawater. *Geophysical Research Letters*, *33*(12). https://doi.org/10.1029/2006GL026011

Leung, J. C.-H., Zhang, B., Gan, Q., Wang, L., Qian, W., & Hu, Z.-Z. (2022). Differential expansion speeds of Indo-Pacific warm pool and deep convection favoring pool under greenhouse warming. *Npj Climate and Atmospheric Science*, *5*(1), 1–15. https://doi.org/10.1038/s41612-022-00315-w

L'Heureux, M. L., Lee, S., & Lyon, B. (2013). Recent multidecadal strengthening of the Walker circulation across the tropical Pacific. *Nature Climate Change*, *3*(6), 571–576. Article 6. https://doi.org/10.1038/nclimate1840

Li, G., Zhang, Y., Xiao, J., Song, X., Abraham, J., Cheng, L., & Zhu, J. (2019). Examining the salinity change in the upper Pacific Ocean during the Argo period. *Climate Dynamics*, *53*(9), 6055–6074. https://doi.org/10.1007/s00382-019-04912-z

Linsley, B. K., Kaplan, A., Gouriou, Y., Salinger, J., de Menocal, P. B., Wellington, G. M., & Howe, S. S. (2006). Tracking the extent of the South Pacific Convergence Zone since the early 1600s. *Geochemistry, Geophysics, Geosystems*, *7*(5). https://doi.org/10.1029/2005GC001115

Linsley, B. K., Wellington, G. M., & Schrag, D. P. (2000). Decadal Sea surface temperature variability in the subtropical South Pacific from 1726 to 1997 A.D. *Science*, *290*(5494), 1145–1148. https://doi.org/10.1126/science.290.5494.1145

Linsley, B. K., Wellington, G. M., Schrag, D. P., Ren, L., Salinger, M. J., & Tudhope, A. W. (2004). Geochemical evidence from corals for changes in the amplitude and spatial pattern of South Pacific interdecadal climate variability over the last 300 years. *Climate Dynamics*, *22*(1), 1–11. https://doi.org/10.1007/s00382-003-0364-y

Linsley, B. K., Wu, H. C., Dassié, E. P., & Schrag, D. P. (2015). Decadal changes in South Pacific Sea surface temperatures and the relationship to the Pacific decadal oscillation and upper ocean heat content. *Geophysical Research Letters*, *42*(7), 2358–2366. https://doi.org/10.1002/2015GL063045

Linsley, B. K., Zhang, P., Kaplan, A., Howe, S. S., & Wellington, G. M. (2008). Interdecadal-decadal climate variability from multicoral oxygen isotope records in the South Pacific Convergence Zone region since 1650 A.D.. *Paleoceanography*, *23*(2). https://doi.org/10.1029/2007PA001539

Liu, X., & Grise, K. M. (2023). Implications of warm pool bias in CMIP6 models on the northern Hemisphere wintertime subtropical jet and precipitation. *Geophysical Research Letters*, *50*(15), e2023GL104896. https://doi.org/10.1029/2023GL104896

Liu, Z., & Huang, B. (1997). A coupled theory of tropical climatology: Warm pool, cold tongue, and Walker circulation. *Journal of Climate*, *10*(7), 1662–1679. https://doi.org/10.1175/1520-0442(1997)010<1662:ACTOTC>2.0.CO;2

Marshall, J. F., & McCulloch, M. T. (2002). An assessment of the Sr/Ca ratio in shallow water hermatypic corals as a proxy for sea surface temperature. *Geochimica et Cosmochimica Acta*, *66*(18), 3263–3280. https://doi.org/10.1016/S0016-7037(02)00926-2

McGree, S., Schreider, S., & Kuleshov, Y. (2016). Trends and variability in droughts in the Pacific islands and northeast Australia. *Journal of Climate*, *29*(23), 8377–8397. https://doi.org/10.1175/JCLI-D-16-0332.1

Mitsuguchi, T., Matsumoto, E., & Uchida, T. (2003). Mg/Ca and Sr/Ca ratios of *Porites* coral skeleton: Evaluation of the effect of skeletal growth rate. *Coral Reefs*, *22*(4), 381–388. https://doi.org/10.1007/s00338-003-0326-1

Nurhati, I. S., Cobb, K. M., & Di Lorenzo, E. (2011). Decadal-scale SST and salinity variations in the central tropical Pacific: Signatures of natural and anthropogenic climate change. *Journal of Climate*, *24*(13), 3294–3308. https://doi.org/10.1175/2011JCLI3852.1

Okai, T., Suzuki, A., Kawahata, H., Terashima, S., & Imai, N. (2002). Preparation of a new geological survey of Japan geochemical reference material: Coral JCp-1. *Geostandards and Geoanalytical Research*, *26*(1), 95–99. https://doi.org/10.1111/j.1751-908X.2002.tb00627.x

Oliver, T. A., & Palumbi, S. R. (2011). Do fluctuating temperature environments elevate coral thermal tolerance? *Coral Reefs*, *30*(2), 429–440. https://doi.org/10.1007/s00338-011-0721-y

Peter, R., Kuttippurath, J., Chakraborty, K., & Sunanda, N. (2023). A high concentration CO_2 pool over the Indo-Pacific Warm Pool. *Scientific Reports*, *13*(1), 4314. Article 1. https://doi.org/10.1038/s41598-023-31468-0

Pfeiffer, M., Dullo, W.-C., Dullo, W.-C., Zinke, J., & Garbe-Schönberg, C.-D. (2009). Three monthly coral Sr/Ca records from the Chagos Archipelago covering the period of 1950–1995 A.D.: Reproducibility and implications for quantitative reconstructions of sea surface temperature variations. *International Journal of Earth Sciences*, *98*(1), 53–66. https://doi.org/10.1007/s00531-008-0326-z

Quinn, T. M., & Sampson, D. E. (2002). A multiproxy approach to reconstructing sea surface conditions using coral skeleton geochemistry. *Paleoceanography*, *17*(4), 14-1. https://doi.org/10.1029/2000PA000528

Quinn, T. M., Taylor, F. W., & Crowley, T. J. (2006). Coral-based climate variability in the western Pacific warm pool since 1867. *Journal of Geophysical Research*, *111*(11). https://doi.org/10.1029/2005jc003243

Ray, S., & Giese, B. S. (2012). Historical changes in El Niño and La Niña characteristics in an ocean reanalysis. *Journal of Geophysical Research*, *117*(C11). https://doi.org/10.1029/2012JC008031

Rayner, N., Parker, D. E., Horton, E. B., Folland, C. K., Alexander, L. V., Rowell, D. P., et al. (2003). Global analyses of sea surface temperature, sea ice, and night marine air temperature since the late nineteenth century. *Journal of Geophysical Research*, *108*(D14), 4407. https://doi.org/10.1029/2002jd002670

R Core Team. (2021). R foundation for statistical computing [Computer software]. https://www.R-project.org/

Ren, L., Linsley, B. K., Wellington, G. M., Schrag, D. P., & Hoegh-Guldberg, O. (2002). Deconvolving the $\delta^{18}O$ seawater component from subseasonal coral $\delta^{18}O$ and Sr/Ca at Rarotonga in the southwestern subtropical Pacific for the period 1726 to 1997. *Geochimica et Cosmochimica Acta*, *67*(9), 1609–1621. https://doi.org/10.1016/S0016-7037(02)00917-1

Reynolds, R. W., Rayner, N., Smith, T. M., Stokes, D. C., Wang, W., & Wang, W. (2002). An improved in situ and satellite SST analysis for climate. *Journal of Climate*, *15*(13), 1609–1625. https://doi.org/10.1175/1520-0442(2002)015<1609:aiisas>2.0.co;2

Roxy, M. K., Dasgupta, P., McPhaden, M. J., Suematsu, T., Zhang, C., & Kim, D. (2019). Twofold expansion of the Indo-Pacific warm pool warps the MJO life cycle. *Nature*, *575*(7784), 647–651. Article 7784. https://doi.org/10.1038/s41586-019-1764-4

Safaie, A., Silbiger, N. J., McClanahan, T. R., Pawlak, G., Barshis, D. J., Hench, J. L., et al. (2018). High frequency temperature variability reduces the risk of coral bleaching. *Nature Communications*, *9*(1), 1671. Article 1. https://doi.org/10.1038/s41467-018-04074-2

Salinger, M. J., Basher, R. E., Fitzharris, B. B., Hay, J. E., Jones, P. D., Macveigh, J. P., & Schmidely-Leleu, I. (1995). Climate trends in the South-West Pacific. *International Journal of Climatology*, *15*(3), 285–302. https://doi.org/10.1002/joc.3370150305

Salinger, M. J., McGree, S., Beucher, F., Power, S. B., & Delage, F. (2014). A new index for variations in the position of the South Pacific Convergence Zone 1910/11–2011/2012. *Climate Dynamics*, *43*(3–4), 881–892. https://doi.org/10.1007/s00382-013-2035-y

Schmidt, G. A. (1999). Forward modeling of carbonate proxy data from planktonic foraminifera using oxygen isotope tracers in a global ocean model. *Paleoceanography*, *14*(4), 482–497. https://doi.org/10.1029/1999PA900025

Schoepf, V., D'Olivo, J. P., Rigal, C., Jung, E. M. U., & McCulloch, M. T. (2021). Heat stress differentially impacts key calcification mechanisms in reef-building corals. *Coral Reefs*, *40*(2), 459–471. https://doi.org/10.1007/s00338-020-02038-x

Schrag, D. P. (1999). Rapid analysis of high-precision Sr/Ca ratios in corals and other marine carbonates. *Paleoceanography*, *14*(2), 97–102. https://doi.org/10.1029/1998PA900025

Schwarz, G. (1978). Estimating the dimension of a model. *Annals of Statistics*, *6*(2), 461–464. https://doi.org/10.1214/aos/1176344136

Seager, R., Cane, M., Henderson, N., Lee, D.-E., Abernathey, R., & Zhang, H. (2019). Strengthening tropical Pacific zonal sea surface temperature gradient consistent with rising greenhouse gases. *Nature Climate Change*, *9*(7), 517–522. Article 7. https://doi.org/10.1038/s41558-019-0505-x

Seager, R., & Murtugudde, R. (1997). Ocean dynamics, thermocline adjustment, and regulation of tropical SST. *Journal of Climate*, *10*(3), 521–534. https://doi.org/10.1175/1520-0442(1997)010<0521:ODTAAR>2.0.CO;2

Shi, X., Beaulieu, C., Killick, R., & Lund, R. (2022). Changepoint detection: An analysis of the central England temperature series. *Journal of Climate*, *35*(19), 6329–6342. https://doi.org/10.1175/JCLI-D-21-0489.1

Singh, A., Delcroix, T., & Cravatte, S. (2011). Contrasting the flavors of El Niño-Southern Oscillation using sea surface salinity observations. *Journal of Geophysical Research*, *116*(C6), C06016. https://doi.org/10.1029/2010JC006862

Singh, P., Chowdary, J. S., & Gnanaseelan, C. (2013). Impact of prolonged La Niña events on the Indian Ocean with a special emphasis on southwest Tropical Indian Ocean SST. *Global and Planetary Change*, *100*, 28–37. https://doi.org/10.1016/j.gloplacha.2012.10.010

Solow, A. R., & Huppert, A. (2004). A potential bias in coral reconstruction of sea surface temperature. *Geophysical Research Letters*, *31*(6), 2003GL019349. https://doi.org/10.1029/2003GL019349

Tachikawa, K., Timmermann, A., Vidal, L., Sonzogni, C., & Timm, O. E. (2014). CO_2 radiative forcing and Intertropical Convergence Zone influences on western Pacific warm pool climate over the past 400 ka. *Quaternary Science Reviews*, *86*, 24–34. https://doi.org/10.1016/j.quascirev.2013.12.018

Tangri, N., Dunbar, R. B., Linsley, B. K., & Mucciarone, D. M. (2018). ENSO's shrinking twentieth-century footprint revealed in a half-millennium coral core from the South Pacific Convergence Zone. *Paleoceanography and Paleoclimatology*, *33*(11), 1136–1150. https://doi.org/10.1029/2017PA003310

Thompson, D. M., Ault, T. R., Evans, M. N., Cole, J. E., & Emile-Geay, J. (2011). Comparison of observed and simulated tropical climate trends using a forward model of coral $\delta^{18}O$. *Geophysical Research Letters*, *38*(14), n/a-n/a. https://doi.org/10.1029/2011GL048224

Thompson, D. M., Conroy, J. L., Konecky, B. L., Stevenson, S., DeLong, K. L., McKay, N., et al. (2022). Identifying hydro-sensitive coral $\delta^{18}O$ records for improved high-resolution temperature and salinity reconstructions. *Geophysical Research Letters*, *49*(9). https://doi.org/10.1029/2021GL096153

Todorovic, S., Dissard, D., Linsley, B. K., Kuhnert, H., & Wu, H. C. (2024). Paired $\delta^{18}O$ and Sr/Ca, and reconstructed $\delta^{18}O_{sw}$ records of *Porites* sp. from Rotuma (RO2) and Tonga (TNI2), Southwest Pacific [Dataset]. *PANGAEA*. https://doi.org/10.1594/PANGAEA.965772

Trenberth, K. E. (1976). Spatial and temporal variations of the Southern Oscillation. *Quarterly Journal of the Royal Meteorological Society*, *102*(433), 639–653. https://doi.org/10.1002/qj.49710243310

van Hooidonk, R., & Huber, M. (2009). Equivocal evidence for a thermostat and unusually low levels of coral bleaching in the Western Pacific Warm Pool. *Geophysical Research Letters*, *36*(6). https://doi.org/10.1029/2008GL036288

Vecchi, G. A., Clement, A., & Soden, B. J. (2008). Examining the tropical Pacific's response to global warming. *Eos, Transactions American Geophysical Union*, *89*(9), 81–83. https://doi.org/10.1029/2008EO090002

Vincent, E. M., Lengaigne, M., Menkes, C. E., Jourdain, N. C., Marchesiello, P., & Madec, G. (2011). Interannual variability of the South Pacific Convergence Zone and implications for tropical cyclone genesis. *Climate Dynamics*, *36*(9), 1881–1896. https://doi.org/10.1007/s00382-009-0716-3

Weber, J. N., & Woodhead, P. M. J. (1972). Temperature dependence of oxygen-18 concentration in reef coral carbonates. *Journal of Geophysical Research (1896-1977)*, *77*(3), 463–473. https://doi.org/10.1029/JC077i003p00463

Weller, E., Min, S.-K., Cai, W., Zwiers, F. W., Kim, Y.-H., & Lee, D. (2016). Human-caused Indo-Pacific warm pool expansion. *Science Advances*, *2*(7), e1501719. https://doi.org/10.1126/sciadv.1501719

Wolter, K., & Timlin, M. S. (2011). El Niño/Southern Oscillation behaviour since 1871 as diagnosed in an extended multivariate ENSO index (MEI.ext). *International Journal of Climatology*, *31*(7), 1074–1087. https://doi.org/10.1002/joc.2336

Wu, H. C., Linsley, B. K., Dassié, E. P., Schiraldi, B., & de Menocal, P. B. (2013). Oceanographic variability in the South Pacific Convergence Zone region over the last 210 years from multi-site coral Sr/Ca records. *Geochemistry, Geophysics, Geosystems*, *14*(5), 1435–1453. https://doi.org/10.1029/2012GC004293

Xie, S.-P., Deser, C., Vecchi, G. A., Ma, J., Teng, H., & Wittenberg, A. T. (2010). Global warming pattern formation: Sea surface temperature and rainfall. *Journal of Climate*, *23*(4), 966–986. https://doi.org/10.1175/2009JCLI3329.1

Yasunaka, S., & Hanawa, K. (2011). Intercomparison of historical sea surface temperature dataset. *International Journal of Climatology*, *31*(7), 1056–1073. https://doi.org/10.1002/joc.2104